# A Standard Set of Pericyclic Reactions of Hydrocarbons for the Benchmarking of Computational Methods: The Performance of ab Initio, Density Functional, CASSCF, CASPT2, and CBS-QB3 Methods for the Prediction of Activation Barriers, Reaction Energetics, and Transition State Geometries

**Vildan Guner,**[†] **Kelli S. Khuong, Andrew G. Leach, Patrick S. Lee, Michael D. Bartberger, and K. N. Houk***

*Department of Chemistry and Biochemistry, University of California, Los Angeles, Los Angeles, California 90095-1569*

Experimental and theoretical data are provided for a set of 11 pericyclic reactions of unsaturated hydrocarbons. Literature experimental data are evaluated and standardized to $\Delta H^{\ddagger}_{0K}$ for comparison to theory. Hartree−Fock, MP2, CASSCF, CASPT2, density functional theory (B3LYP, BPW91, MPW1K, and KMLYP functionals), and CBS-QB3 transition-structure geometries, activation enthalpies and entropies, and reaction enthalpies and entropies for these reactions are reported and are compared to experimental results. For activation enthalpies, several density functionals rival CASPT2 and CBS-QB3 for closest agreement with experiment, while CASPT2 and CBS-QB3 provide the most accurate heats of reaction. Transition-structure geometries are reproduced well by all methods with the exception of the Cope rearrangement and cyclopentadiene dimerization transition structures.

## Introduction

The development of computational methods for the exploration of chemical thermodynamics has been facilitated by the assembly of reliable sets of experimental data that can be used to evaluate, or to calibrate, theoretical methods.[1] The G1, G2, and G3 data sets of atomization energies, ionization energies, electron affinities, and proton affinities from Curtiss et al. are perhaps the best known.[2] Other sets of evaluated data and computational method benchmarks are available for heats of formation for organic radicals.[3]

These experimental data have provided means to determine how well different computational methods perform. Statistical analyses such as those summarized in the tables and figures of Foresman and Frisch[4] permit the choice of a method that balances speed with cost and accuracy. The data set has proven of special value for the development of new density functionals[5] and extrapolation procedures such as Peterssons' CBS[6] and Martin's Wn methods.[7] No similarly extensive set of data exists for activation enthalpies, although recent examples of limited types of reactions have been reported and are summarized here.

We have undertaken a general program to provide critically evaluated experimental activation barriers and to test the performance of different levels of theory for the calculations of such barriers. Our initial efforts involve hydrocarbon pericyclic reactions, a field where we have had extensive experience and have already reported many computational investigations.[8,9] Such reactions are known to have relatively minor variational effects that might cause computed classical activation barriers to differ from experimental barriers.[8,10] Furthermore, gas-phase data are available, and solvation usually has a very small effect

on barriers. Kinetic isotope effects have been measured for a number of pericyclic reactions, and theory (particularly at the B3LYP density functional level) has been remarkably successful at reproducing these experimental results.[11] This signals that the method accurately predicts vibrational frequency changes and, presumably, geometry changes between reactant and transition structure.

The pericyclic reactions chosen for our initial data set are shown in Figure 1. These are reactions for which the evidence indicates that concerted mechanisms operate. Our goals are (a) to provide a set of reliable experimental activation enthalpies for benchmarking, (b) to establish the level of theory necessary to give highly accurate activation enthalpies, and (c) to establish a practical level of density-functional theory (DFT) to be used for the exploration of organic reactions.

The organization of this paper is as follows. First, previous studies that benchmark computations of activation enthalpies of reactions are reviewed. Next, the experimental data available for 11 typical hydrocarbon pericyclic reactions are summarized and critically evaluated. Third, the theoretical methods chosen for analysis are described. Fourth, predicted activation enthalpies and reaction enthalpies are compared with experimental data, and the results are analyzed statistically and graphically. Finally, some apparent difficulties with a few of the experimental quantities are discussed, and final recommendations as to the most accurate experimental values are given.

## Background

This section surveys recent comparisons of theoretical predictions, especially those involving various density functional theory methods, to experimental activation barriers.

Truhlar reported studies for a set of 22 reactions mainly involving hydrogen atom transfer to radicals. Comparison of MPW1K (modified Perdew−Wang one-parameter model for

---

* Author to whom correspondence should be addressed. E-mail: houk@chem.ucla.edu.

† Permanent address. Department of Chemistry, Hacettepe University, 06532, Beytepe, Ankara, Turkey.

**11446** *J. Phys. Chem. A, Vol. 107, No. 51, 2003*

Guner et al.
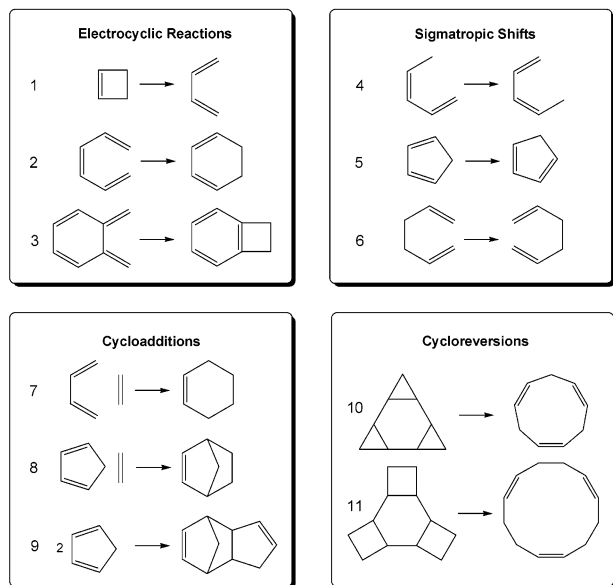
**Figure 1.** Set of 11 pericyclic reactions of hydrocarbons used for benchmarking.

kinetics) with the other hybrid Hartree−Fock (HF)-DFT methods[12] and ab initio methods, MP2 and QCISD[13] reveals that MPW1K provides very accurate results. Using the same data set, they evaluated the accuracy and cost of multicoefficient correlation methods (MCG3 and MC-QCISD), MP2, QCISD, and MPW1K.[14] MPW1K is as good as MC-QCISD and MCG3 in accuracy. Most recently, Lynch and Truhlar have fine tuned several multicoefficient correlation methods versus an experimental data set. Several multicoefficient correlation methods, CBS-Q, and G3 give accurate barriers, while MPW1K performs best of the tested density functional methods.[15]

Kang and Musgrave explored transition-state barriers and enthalpies of reaction for a set including 46 hydrogen atom transfer reactions and 28 non-hydrogen atom abstraction reactions by the KMLYP, G2, B3LYP, CBS-APNO, and BH and HLYP methods.[16] The new Kang−Musgrave functional, KM-LYP, was found to be more accurate than either the G2 or B3LYP methods for these reactions and has the same accuracy as CBS-APNO.

Senosiain et al. studied the C−H bond dissociations of 59 hydrocarbons using the KMLYP, B3LYP, and CBS-Q methods. While in most cases B3LYP underestimates the bond dissociation energies, the new KMLYP method gave smaller deviations that were close to those obtained by the CBS-Q method.[17]

While attention has focused on atom and group transfer reaction, benchmarks have been established for some other types of reactions. Martin et al. explored a set of 6 $S_N2$ reactions ($Y^-$ + MeY, where X and Y = F, Cl, or Br) with about 22 different methods ranging from B3LYP/cc-pVTZ(+X) to "W2", a so-called "benchmark accuracy" method that generally gives thermochemistry within 1 kJ/mol of experimental values.[18] As expected, multiparameter methods such as G3, CBS-QB3, and W2 gave accurate results, while density functional methods performed adequately but less accurately. MPW1K with extended basis sets was deemed the best of the density functionals.

A variety of other studies of a small number of specific reactions has been reported.[19] Mari et al.[19a] studied reactions of phosphorus ylides ($R_3P=CH_2$) with formaldehyde, and Rice et al.[19b] studied the decomposition of *sym*-triazine $(CHN)_3$ to form 3 HCN molecules. Both studies showed that B3LYP was in reasonable agreement with higher-level calculations. Baker

et al. explored the reaction of HO• with $H_2$ with various methods and concluded that none of the available density functionals represented the barrier accurately.[19c] Durant also explored seven atom-transfer processes with five different density functionals.[19d]

Dinadayalane et al. carried out calculations on Diels−Alder reactions of five-membered cyclic dienes, $(CH)_4X$ (X = $CH_2$, $SiH_2$, O, NH, PH, and S), with ethylene and acetylene using semiempirical levels (AM1 and PM3), ab initio (HF, MP2, MP3), CCSD(T), and hybrid-DFT (B3LYP) calculations.[20] CCSD(T) with the 6-31G* basis set provided accurate activation barriers and reaction enthalpies, while B3LYP gave good agreement with the CCSD(T) results.

Handy has recently developed a series of functionals among which the OLYP and O3LYP have attracted considerable attention.[21,22] During the preparation of this manuscript, Baker and Pulay reported benchmarking these methods against a set of 12 organic reactions, two of which are pericyclic reactions included here. It was concluded that OLYP, a nonhybrid functional that is faster than B3LYP, is more accurate for the calculation of activation barriers.[23]

## Experimental Data for 11 Hydrocarbon Pericyclic Reactions

Table 1 summarizes the experimental thermodynamic parameters and estimated enthalpies of activation at 0 K for the set of 11 pericyclic reactions of unsaturated hydrocarbons shown in Figure 1. The set includes examples from each principal pericyclic class, electrocyclic reactions, cycloadditions and cycloreversions, and sigmatropic shifts. These are prototypes of very common reactions, or are reactions that have attracted special interest in our laboratories in recent years.[8,9] Furthermore, relatively accurate experimental values of activation energies are available, along with mechanistic evidence for the nature of the transition state, frequently from kinetic isotope effects.[11]

All of the experimental data from the literature are included, and a choice has been made as to the most reliable activation energies. The chosen value was corrected to $\Delta H^{\ddagger}_{0K}$ as described later. The measured heats of reaction were averaged to give the best estimate of the heat of reaction.

The thermal isomerization of cyclobutene to butadiene, reaction 1, has been studied in the temperature range 403−448 K, and the measured activation energies range from 30.2 to 32.9 kcal/mol.[24−26] The value of 32.7 ± 0.2 kcal/mol is found at pressures down to 5 mm pressure but falls off to 30.2 ± 0.2 kcal/mol at lower pressures. The value of 32.7 ± 0.2 kcal/mol is used here. The experimental heat of reaction ranges from −11.5 to −9.7 kcal/mol, depending on the butadiene heat of formation used in the calculation, and an average is used in Table 1.[27]

The activation parameters for thermal cyclization of *cis*-hexa-1,3,5-triene, reaction 2, have been measured only once, and an experimental activation energy of 29.9 ± 0.5 kcal/mol was reported for the gas phase at 390−434 K.[30] The heat of reaction has been measured as −14.5 kcal/mol[28] and estimated as −16.1 kcal/mol.[31]

For the ring closure of *o*-xylylene to benzocyclobutene, reaction 3, the activation energy has been measured indirectly by competition with dimerization. The result is 29.3 ± 0.3 kcal/mol at temperatures between 460 and 501 K.[32] The reaction is exothermic by 10.5 kcal/mol. Although the measurements were reproducible, it is suggested later in this manuscript that the activation energy should be revised downward.

The [1,5]-sigmatropic hydrogen shift of 1,3-pentadiene, reaction 4, was measured for *cis*-1,1-dideutero-1,3-pentadiene.

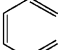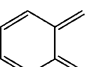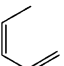## TABLE 1: Experimental Activation and Reaction Enthalpies for 11 Hydrocarbon Pericyclic Reactions[a]
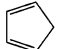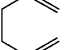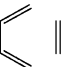
| Reaction | $\Delta H^{\ddagger}$ (kcal/mol) | $E_a$ (kcal/mol) | log A (l-mol/s) | $\Delta S^{\ddagger}$ (cal/molK) | $\Delta H_{rxn}$ (kcal/mol) | $\Delta S_{rxn}$ (cal/molK) | $\Delta H^{\ddagger}_{0K}$ (kcal/mol) | Avg $\Delta H_{rxn}$ (kcal/mol) |
|---|---|---|---|---|---|---|---|---|
| 1 | **31.9**, (426 K) [a] | 32.5 ± 0.5 (g), (403–448 K, 8–14 mmHg) [24]<br>32.5 ± 0.4 (g), (403–448 K, 100 mmHg) [25]<br>32.9 ± 0.7 (g), (403–448 K,1500 mmHg) [25]<br>**32.7 ± 0.2(g), (403–448 K, 5 mmHg) [26]**<br>30.7 ± 0.2 (g), (403–448 K, 0.2 mmHg) [26]<br>30.2 ± 0.2 (g), (423–448 K, 0.06 mmHg) [26] | 13.1 [24]<br>13.4 [25]<br>13.0 [25]<br>13.3 [26]<br>13.2 [26]<br>13.1 [27] | −1.4, (423 K, 1500 mmHg) [24] | −11.5 [27]<br>−10.8 [27]<br>−9.7 [28] | 4.5, (400 K) [29] | *31.9 ± 0.2* | *−10.6 ± 1* |
| 2 | **29.1**, (412 K) [a] | **29.9 ± 0.5 (g), (390–434 K) [30]** | 11.9 [30] | −7.0 [30] | −14.5 [28]<br>−16.1 [31] | −5.9 [28] | *30.2 ± 0.5* | *−15.3 ± 1* |
| 3 | **28.3**, (481 K) [a]<br>28.4 (g), (473K) [32] | **29.3 ± 0.3 (g), (460–501 K) [32]** | 13.3 [32] | 0.39 [32] | −10.5 [32] | | *29.1 ± 0.3* | *−10.5 ± 1* |
| 4 | **35.4**, (468 K) [a]<br>35.4 (g), (473 K) [33,34] | **36.3 ± 0.5 (g), (458–478 K) [33]** | 11.5 [34] | −7.1, (473 K) [33,34] | 0.0 | | *36.7 ± 0.5* | *0.0* |
| 5 | **23.6**, (328 K) [a] | **24.3 ± 0.5 (CCl₄), (318–338 K) [35]** | 12.1 [35] | −5.3 [35] | 0.0 | | *23.7 ± 0.5* | *0.0* |
| 6 | **33.5 ± 0.5, (480–531 K) [36]**<br>33.3, (506 K) [a] | **34.3 (g), (480–531 K) [36]** | 10.4 [36] | −13.8 ± 1 [36] | 0.0 | | *34.5 ± 0.5* | *0.0* |
| 7 | **24.2**, (841 K) [a] | **27.5 ± 0.5 (g), (760–921 K) [37]**<br>26.6 [b] [38]<br>15.5 [c] [39]<br>33.1 [d] [40] | 10.5 | −45.8 [37]<br>−44.7 [38] | −37.9, (800 K) [37]<br>−40.1, (814-902 K) [38]<br><br>−39.6 [41] | | *23.3 ± 2* | |

**TABLE 1:  (Continued)**

|   |   |   |   |   |   |   |
|---|---|---|---|---|---|---|
|   |   |   |   |   | −40.8 [18] |   |
|   |   |   |   |   |   | *−39.6 ± 1* |
| **8** | **22.6**, (546 K) [a] | 23.7 ± 1.6 (g), (521–570 K) [42] | 7.6 ± 0.6, (298 K) [42] | −45.4 [42] |   | *21.6 ± 1.6* |
|   |   | 21.6 [e] [42] | −20.9, (521–570 K) [42] |   |   |   |
|   |   | 19.9 [f] [43] |   |   |   |   |
|   |   | 20.6 [g] [44] |   |   |   |   |
|   |   | 23.4 [h] [45] |   |   |   |   |
|   |   | 21.7 [i] [46] |   |   |   |   |
|   |   |   | −24.9, (560 K) [47] |   | −23.2 ± 0.6 [47] | *−23.2 ± 0.6* |
| **9** |   | 14.9(g), (393–467 K) [48] | 7.9 [48] | −31.5 (g) [48] | −18.8(g) [48] |   |
|   |   | 17.1(l), (273–344 K) [48] |   | −32.5 (l) [48] |   |   |
|   |   | 14.0 [j] [48] |   |   |   |   |
|   | **15.2** (388 K) [a] | **16.7 ± 0.6 (g), (352–423 K)** [50,49] |   |   | −18.4(l) [50] | *15.1 ± 0.6* |
|   |   |   |   |   | −21.4(g) [50] |   |
|   |   |   |   |   | −17. 3(l) [49] |   |
|   |   |   |   |   | −18.8 (g) [49] |   |
|   |   | 16.9 ± 0.5 (g), (405–455 K) [51] | 6.8 [51] |   | −19.7 (g) [51] |   |
|   |   | 17.3 [k] [51] |   |   |   |   |
|   |   | 16.2 ± 0.8 (l) [52] | 6.7 ± 0.3 [52] |   |   |   |
|   |   | 17.1 ± 0.4 (CCl₄) [52] | 5.8 ± 0.5 [52] |   |   |   |
|   |   | 16.5 ± 0.1 (l) (293–438 K) [53] |   |   | −18.8 (l) [53] |   |
|   |   | 15.8 [l] [53] |   |   |   |   |
|   |   | 12.7 (g) [54] |   |   |   |   |
|   |   | 17.3 (l) [54] |   |   |   |   |
|   |   | 14.0 [m] [54] |   |   |   |   |
|   | 13.3 [n] [55] | 14.3 [o] [55] |   |   |   |   |
|   |   |   |   |   |   | *−19.7 (g)* |
|   |   |   |   |   |   | *−18.2 (l)* |
| **10** | 23.4–25.8(g), (298 K) [56] | **24.0–26.4 (g)** [56] | 5.0 [56] |   | 14.3 [56] | *24.4± 3* |
|   | **24.6, (298 K)** [a] |   |   |   |   |   |
| **11** | **50–52 (g), (723–773 K)** [57] |   |   |   |   | *46.5 ± 3* |
|   | **52.5,** (748 K) [a] |   |   |   |   |   |

$^a$ Values in boldface were chosen for the calculation of $\Delta H^{\ddagger}_{0K}$ and taken as the most reliable values. Values in italics were used for comparisons with theory. [a] Experimental $E_a - nRT$, where $T$ is the average experimental temperature and $n$ is 1 for a unimolecular reaction and 2 for a bimolecular reaction. [b] through [o]: $E_a$ of forward reaction is estimated by ($E_a$ of reverse reaction) − (average $\Delta H_{rxn}$). [b] 26.6 = 66.2 kcal/mol (814 − 902 K) − 39.6 kcal/mol; ref 38. [c] 15.5 = 55.1 kcal/mol (938 − 1018 K) − 39.6 kcal/mol; ref 39. [d] 33.1 = 72.7 kcal/mol (719 − 808 K) − 39.6 kcal/mol; ref 40.[e] 21.6 = 44.5 kcal/mol (530 − 570 K) − 22.9 kcal/mol; ref 42. [f] 19.9 = 42.8 kcal/mol (577 − 671 K) − 22.9 kcal/mol; ref 43. [g] 20.6 = 43.5 kcal/mol (539 − 577 K) − 22.9 kcal/mol; ref 44. [h] 23.4 = 46.3 kcal/mol (500 − 1300 K) − 22.9 kcal/mol; ref 45. [i] 21.7 = 44.6 kcal/mol (563 − 618 K) − 22.9 kcal/mol; ref 46. [j] 14.0 = 33.7 kcal/mol (426 − 484 K) − 19.7 kcal/mol; ref 48. [k] 17.3 = 37.0 kcal/mol (352 − 448 K) − 19.7 kcal/mol; ref 51. [l] 15.8 = 34.0 kcal/mol (405 − 455 K) − 18.2 kcal/mol; ref 53. [m] 14.0 = 33.7 kcal/mol (332 K) − 19.7 kcal/mol; ref 54. [n] 13.3 = 33.0 kcal/mol (426 − 484 K) − 19.7 kcal/mol; ref 55. [o] 14.3 = 34.0 kcal/mol (426 − 484 K) − 19.7 kcal/mol; ref 55.

Benchmarking Computational Methods

*J. Phys. Chem. A, Vol. 107, No. 51, 2003* **11449**

Kinetic studies were carried out at 458−478 K in the gas phase. Values of $\Delta H^\ddagger = 35.4$ kcal/mol (473 K), and $\Delta S^\ddagger = -7.1$ kcal/mol were measured.[33,34] Lynch and Truhlar have made an independent estimate of the zero-point-exclusive barrier height to be 38.4 kcal/mol,[13] which would correspond to a $\Delta H^\ddagger_{(0K)}$ of ~36 kcal/mol.[58] Dynamics calculations by Truhlar and coworkers show that hydrogen tunneling influences this barrier and that $\Delta H^\ddagger_{(0K)}$ is ~36 kcal/mol.[58]

The activation energy determined for the [1,5]-sigmatropic shift of deuterium in 1,2,3,4,5-pentadeutero-1,3-cyclopentadiene is 12 kcal/mol lower than that of the acyclic system 1,3-pentadiene. The measured activation energy in CCl$_4$ at 318−338 K is 24.3 ± 0.5 kcal/mol.[35]

Thermodynamic and kinetic parameters for the Cope rearrangement of 1,1-dideuterohexa-1,5-diene to 3,3-dideuterohexa-1,5-diene were studied by Doering et al.[36] The activation enthalpy and entropy are 33.5 ± 0.5 kcal/mol and −13.8 ± 1 eu, respectively.

Gas-phase kinetic studies of the prototype Diels−Alder reaction of butadiene with ethylene to form cyclohexene, reaction 7, were reported by Rowley and Steiner.[37] The activation energy found for this reaction is 27.5 ± 0.5 kcal/mol, and the heat of reaction is −37.9 ± 1 kcal/mol. The heat of reaction was also measured as −40.1 kcal/mol,[38] while a third value of −39.6 kcal/mol[41] was estimated from known heats of formation. When activation energies were estimated using values for the reverse reaction, the activation energies obtained were 15.5,[39] 26.6,[38] and 33.1[40] kcal/mol. The 27.5 kcal/mol value is taken as the best available activation barrier, but we have assigned the error bars on this value to be quite large, ±2 kcal/mol.

The activation energy for the Diels−Alder reaction between cyclopentadiene and ethylene, measured in a static system at temperatures in the range 521−570 K, is 23.7 ± 1.6 kcal/mol.[42] The estimated values from the activation energy and energy of the reverse reactions are between 19.9 and 23.4 kcal/mol.[42−46]

The kinetics of dimerization of cyclopentadiene, reaction 9, were determined by many different groups for the gas and liquid phases.[48−52] The measured activation energies vary between 12.7 and 17.3 kcal/mol depending on the temperature range of the study and on whether the reaction is carried out in gas phase or solution. At temperatures <100 °C, *endo*-dicyclopentadiene is the only reaction product of the liquid cyclopentadiene. However, at pressures above 1 atm or at temperatures >150 °C, higher-order polymers, tri-, tetra-, and pentacyclopentadiene are formed. Activation energies obtained for dimerization of cyclopentadiene in solution are higher in the neat liquid (17.1 kcal/mol)[50] or in tetrahydronaphthalene (17.3 kcal/mol)[48] than in the gas phase (14.9 kcal/mol).[48] Also, the formation of dicyclopentadiene is less exothermic in the condensed phase ($\Delta H_{rxn} = -18.5$ kcal/mol and −21.4 kcal/mol, liquid and gas phases, respectively) because the solvation energy of two cyclopentadienes is greater than that of one dicyclopentadiene. Furthermore, *exo*-dicyclopentadiene is formed from *endo*-dicyclopentadiene at temperatures (150−170 °C) that lie within the range of kinetic studies. Values for the retrocycloaddition have also been used to estimate the activation enthalpy for the forward reaction. We have adopted the intermediate value of 16.6 kcal/mol as the most reliable experimental quantity, although computational results described later suggest that a further downward revision of this barrier is in order.

For the [2 + 2 + 2] cycloreversion of *cis*-triscyclopropano-cyclohexane and *cis*-triscyclobutanocyclohexane, $\Delta H^\ddagger$ values of 23.4−25.8 and 50−52 kcal/mol were estimated, respec-

tively.[56,57] Both of these involve rather large presumptions and are likely to have errors of ±3 kcal/mol. For example, the de Meijere group estimated the cycloreversion activation energy of *cis*-tris-cyclopropanocyclohexane, **1**, by comparing the measured activation energies of compounds **2** and **3**.[56] The difference in activation energies of **2** and **3** was taken to be the energy difference in going from three strained bridged cyclopropanes to two strained bridged cyclopropanes. This difference was multiplied by three to estimate the difference between the activation energy of **2** and that of the unbridged **1**. For the triscyclobutano compound, the activation energy was estimated by the authors to be about 50 kcal/mol based on the onset of reaction at 673 K and the percent conversion to product as the temperature was increased to 773 K.[57] The heats of reaction have not been measured for either reaction 10 or 11. Since the [2 + 2 + 2] reactions have large errors, the theoretical methods were tested both vs the whole data set and with these two reactions excluded.



**1**          **2**          **3**
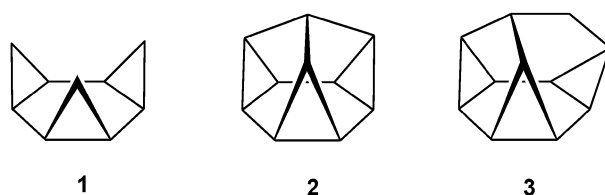
## Determination of $\Delta H^\ddagger_{0K}$ Values

Quantum mechanical calculations provide predicted data for isolated molecules at 0 K with stationary nuclei, while experimental thermochemical measurements are carried out at finite temperatures. We assume the validity of transition-state theory and obtain $\Delta H^\ddagger_{0K}$ by subtracting the thermal corrections (Cp*T) for transition structures and reactants obtained from quantum mechanical calculations from the experimental activation enthalpies, as described below. These calculations use harmonic potentials to obtain vibrational frequencies. In addition to errors that might arise from anharmonicity of the vibrational potentials, deviations from transition-state theory can arise from tunneling, re-crossing, and variational effects. We have neglected these in our treatment.

We chose to compare computed data (electronic energy plus a zero-point energy correction at 0 K) with experimental data corrected to 0 K. Experimental data at different temperature ranges were corrected to 0 K by subtracting the theoretically derived thermal corrections from the experimental activation enthalpy

$$\Delta H^\ddagger_{0K(exp)} = (\Delta H^\ddagger_{T(exp)} - (TCE)_{TS} + (TCE)_R)$$

TCE is the thermal correction of enthalpy for the transition structure (TS) and reactant (R) obtained from B3LYP/6-31G* frequency calculations. This thermal correction comes from the computed heat capacity, assumed to be approximately temperature independent and computed from the harmonic frequencies of Gaussian98.[59] For three of these reactions, we also tested the thermal corrections obtained from frequencies calculated by other methods (Table 2). The results are in agreement to within 0.4 kcal/mol, which is considerably less than experimental error for most cases. Therefore, the final values of $\Delta H^\ddagger_{0K}$ are not highly dependent on the basis set or the method of computing the thermal correction.

## Computational Methods Evaluated

The methods studied here were chosen for several reasons. HF was long the standard for ab initio computational chemistry

**11450** *J. Phys. Chem. A, Vol. 107, No. 51, 2003*

Guner et al.

**TABLE 2: Estimated $\Delta H^{\ddagger}_{0K}$ (kcal/mol) at Using Different Methods for Thermal Corrections for Reactions 2, 5, and 8**

| methods | reaction 2 | reaction 5 | reaction 8 |
|---|---|---|---|
| HF/6-31G* | 30.3 | 23.9 | 23.2 |
| B3LYP/6-31G* | 30.4 | 23.9 | 22.9 |
| B3LYP/6-31+G** | 30.4 | 23.9 | 22.9 |
| MP2/6-31G* | 30.4 | 23.9 | 23.0 |
| BPW91/6-31G* | 30.4 | 23.9 | 22.8 |
| MPW1K/6-31+G** | 30.4 | 23.9 | 22.9 |

and, especially applied to isodesmic reactions, can give accurate thermodynamics.[60,61] Since the HF method neglects electron correlation, the calculated activation enthalpies are systematically too high because the correlation energy of the transition structure is much greater than for reactants. Nevertheless, the method can be quite accurate for heats of reaction and useful for relative activation barriers.

Other ab initio methods include MP2, CASSCF, and CASPT2, although CASSCF and CASPT2 have arbitrariness due to the necessity for choice of the active space to be used in the calculation. Møller−Plesset second-order perturbation theory (MP2)[60,62] includes electron-correlation energy through a second-order perturbation estimate. The calculated activation enthalpies are often too low, since the MP2 method overestimates correlation energies, and these increase from reactant to transition structure. MP2 is generally considered to give accurate geometries and is typically used to obtain geometries for the Gn methods.[2]

CASSCF (complete active space SCF)[63] is a multiconfigurational SCF method that has proven useful for the study of organic chemical reactions. It provides an appropriate description of open-shell minima or transition structures due to its inclusion of nondynamical electron correlation.[64,65] CASSCF is a combination of SCF computation with a full configuration interaction for all active electrons. When dynamical correlation is also computed with second-order perturbation theory,[65] the method is referred to as CASPT2.[66] Calculations up to about 12−15 active orbitals have been performed with this method. These highly correlated methods are often used for single-point energy calculations of structures that have been optimized at a lower of theory. As noted before, CASSCF methods are ab initio in the sense of having no arbitrary parameters, although an arbitrary, but usually reasonable, choice of active space must be made.

DFT methods have provided surprising and important efficiency in quantum mechanical computation of reaction barriers and enthalpies of reaction. On the basis of the Kohn−Sham theorem[67a] that energy is a functional of electron density, very efficient methods including all electron correlation have been developed. Hybrid DFT methods involve mixing various amounts of the HF exact exchange with DFT exchange correlation functionals. Since the exact functional is not known, various functionals that include parameters set to fit experimental data have been developed. Many different exchange[67] and correlation functionals[68] have been proposed, leading to a variety of DFT methods.[69] None are, strictly speaking, ab initio, because of the parameters included in the functional.

The B3LYP functional is based on the Becke three-parameter exchange-correlation functional[70] to which the Lee−Yang−Parr correlation functional (LYP) was added and implemented into the Gaussian program by Frisch et al.[71] The computational cost of B3LYP calculations scales similarly to HF theory with the size of the molecule, but unlike HF theory, electron correlation is accounted for. B3LYP yields good results for both geometries and zero-point vibrational energy corrections.

BPW91 includes Becke's 1988 functional[67b] and the exchange component from Perdew and Wang's 1991 functional.[72]

MPW1K was developed by Truhlar et al.[12−15] It has been recommended that the 6-31+G** basis set[73] be used for MPW1K.[12]

KMLYP is a newly developed hybrid DFT method.[16,17] The correlation functional is a mixture of Vosko−Wilk−Nusair (VWN) and LYP correlations. The combination of VWN and LYP functionals is said to reduce the correlation energy error.

The complete basis set (CBS) methods developed by Petersson involve extrapolations to a complete basis set and complete correlation through a series of calculations and some empirical corrections for different bond types.[6] The CBS method is similar in spirit to Pople et al.'s Gn[2] and Martin's Wn[7] methods. In the CBS-QB3 model used here, CBS-Q energy calculations are combined with B3LYP/CBSB7-optimized geometries and frequencies. The five-step series of calculations starts with a geometry optimization at the B3LYP level, followed by a frequency calculation to obtain thermal corrections, zero-point vibrational energy, and entropic information. The next three calculations are single-point calculations at the CCSD(T), MP4SDQ, and MP2 levels. The CBS extrapolation then gives final energies.

**Computational Procedures**

Calculations using HF, MP2, density functional theory with four functionals (B3LYP, BPW91, KMLYP, and MPW1K), CASSCF, and CBS-QB3 were performed with Gaussian 98.[59] CASPT2 energies were computed using the method of Roos et al.[74] with the MOLCAS suite of ab initio programs.[75]

Initially, the structures of all of the reactants, transition structures, and products were optimized using HF, MP2, BPW91, B3LYP, KMLYP, and CASSCF with the 6-31G* basis set,[76] B3LYP and MPW1K with the 6-31+G** basis, and KMLYP with the 6-311G basis set. All of the reactants and products were characterized as minima, and the saddle points were proved to be first-order transition structures by frequency calculations. All the activation enthalpies reported are corrected for zero-point energy (ZPE) at 0 K. The computed ZPEs were scaled by 0.9135, 0.9804, 0.9646, and 0.9515 for HF/6-31G*, B3LYP/6-31G*, MP2/6-31G*, and MPW1K/6-31+G**, respectively.[4,8] Zero-point correction factors for B3LYP/6-31+G**, CASSCF/6-31G*, KMLYP/6-31G*, and KMLYP/6-311G were not scaled. CASPT2 single point calculations were performed for both B3LYP/6-31G* and CASSCF/6-31G* optimized geometries. The active space for CASSCF and CASPT2 calculations includes four electrons in four orbitals for reactions 1 and 4−9, six electrons in six orbitals for reactions 2, 10, and 11, and eight electrons in eight orbitals for reaction 3. The reported CASPT2 values include either the scaled B3LYP/6-31G* ZPE corrections or the unscaled CASSCF ZPE corrections, depending on whether B3LYP or CASSCF geometries were used.

The computed enthalpies of activation ($\Delta H^{\ddagger}_{0K}$), enthalpies of reaction ($\Delta H_{rxn,0K}$), entropies of activation ($\Delta S^{\ddagger}_{0K}$), and entropies of reaction ($\Delta S_{rxn,0K}$) for 11 pericyclic reactions of hydrocarbons are given in Table 3. Literature values are included here for comparison when these are available. B3LYP/6-31G*-optimized transition structures for 11 pericyclic reactions are depicted in Figure 2. These will be compared with geometries obtained by other methods later in this paper.

Benchmarking Computational Methods

*J. Phys. Chem. A, Vol. 107, No. 51, 2003* **11451**

**TABLE 3: Computed Enthalpies of Activation ($\Delta H^{\ddagger}_{0K}$)*, Entropies of Activation ($\Delta S^{\ddagger}_{0K}$), Energies of Reaction ($\Delta H_{rxn,0K}$), and Entropies of Reaction ($\Delta S_{rxn,0K}$) for 11 Pericyclic Reactions of Hydrocarbons, from the Literature or Reported Here**

| theory | | 1 | 2 | 3 | 4 | 5 | 6 | 7 | 8 | 9 | 10 | 11 |
|---|---|---|---|---|---|---|---|---|---|---|---|---|
| | | | | | | | | reaction | | | | |
| HF/6-31G* | $\Delta H^{\ddagger}$ | 45.3 | 46.8 (45.9)[9e] | 40.9 | 56.7 (58.7)[9g,77,78] | 36.7 (38.8)[79] | 56.0 56.6[80] 55.0[80] | 47.5[9t,9g'] 47.5[81,82] (45.0)[8,82,83] | 42.0 (39.7)[84] | 42.7 | 43.0 | 79.9 |
| | $\Delta S^{\ddagger}$ | −0.08 | −5.8 | −3.8 | −7.0 | −1.1 | | −42.2 | −43.2 | −47.5 | 1.3 | 5.6 |
| | $\Delta H_{rxn}$ | −13.5 | −14.2 | −14.9 | 0.0 | 0.0 | 0.0 | −36.6[9h] | −18.4 | −13.2 | −22.3 | −15.3 |
| | $\Delta S_{rxn}$ | 2.2 | −7.6 | −5.1 | 0.0 | 0.0 | 0.0 | −44.9 | −46.3 | −51.2 | 5.1 | 13.9 |
| MP2/6-31G* | $\Delta H^{\ddagger}$ | 35.8 | 27.2 (26.9)[9e] | 22.9 | 35.9[85,86] (37.7)[9g,86,87] | 26.9 26.4[79,87] (28.6)[79] | 28.5 (28.5) [[33.4]][88] | 20.0[9t,9g'] 20.2[89,90,91] (17.9)[82,83] (17.6)[8,91] | 14.2 14.1[89] (11.8)[9f'] | 7.5 | 21.3 | 52.5 |
| | $\Delta S^{\ddagger}$ | −0.2 | −5.6 | −3.4 | −6.7 | −1.2 | −11.3 | −41.0 | −42.3 | −46.3 | −0.1 | 5.9 |
| | $\Delta H_{rxn}$ | −9.1 | −18.6 | −20.1 | 0.0 | 0.0 | 0.0 | −45.9[8t] | −30.4 | −27.4 | −12.3 | −2.0 |
| | $\Delta S_{rxn}$ | 2.3 | −8.2 | −2.9 | 0.0 | 0.0 | 0.0 | −45.2 | −46.4 | −51.4 | 3.4 | 14.7 |
| CASSCF/6-31G* | $\Delta H^{\ddagger}$ | 34.0 | 44.4 | 35.8 | 47.9 | 40.7 | 47.6 47.7* (48.7)[80] [46.9][80] | 47.0 (43.8)[9i',9q,82,83] 47.4[8t] | 43.2 (38.4)[9h'] | 40.6 (39.5)[99] | 26.1[100,101] (29.4) | 54.9 (59.2)[100,101] |
| | $\Delta S^{\ddagger}$ | −1.9 | −5.8 | −3.8 | −7.2 | −1.3 | −7.0 | −42.5 | −42.5 | −45.3 | 2.9 | 4.9 |
| | $\Delta H_{rxn}$ | −20.4 | −6.8 | −0.2 | 0.0 | 0.0 | 0.0 | −19.0 | −2.9 | −0.9 (−7.6)[99] | −44.2 (−42.0) | −36.7 (−32.4) |
| | $\Delta S_{rxn}$ | 5.1 | −7.7 | −6.3 | 0.0 | 0.0 | 0.0 | −46.4 | −46.5 | −51.4 | 6.0 | 0.0 |
| CASSCF/6-31G** | $\Delta H^{\ddagger}$ | (52.5)[92] | (36.7)[93] | (36.8)[94] | | | | 44.5[95] | | | | |
| | $\Delta H_{rxn}$ | (−16.3)[92] | (−16.7)[93] | (−1.8)[94] | | | | −21.0 | | | | |
| CAS-MP2/6-311+G** | $\Delta H^{\ddagger}$ | (39.1)[92] | (37.2)[93] | (34.9)[94] | | | | 40.9[95] | | | | |
| | $\Delta H_{rxn}$ | (−9.9)[92] | (−23.6)[93] | (−8.0)[94] | | | | −42.5 | | | | |
| CASPT2/6-31G*//B3LYP/6-31G* | $\Delta H^{\ddagger}$ | 33.9 | 30.3 | 24.7 | 37.7 | 28.8 | 33.2 | 27.4 | 17.6 | 12.1 | 25.6 | 55.2 |
| | $\Delta H_{rxn}$ | −11.3 | −16.4 | −13.5 | 0.0 | 0.0 | 0.0 | −41.9 | −27.9 | −26.5 | −14.9 | −5.0 |
| CASPT2/6-31G*//CAS-6-31G* | $\Delta H^{\ddagger}$ | 33.7 | 30.9 | 25.4 | 37.7 | 29.4 | 35.9 | 25.0 | 18.6 | 12.7 | 24.3 | 54.3 |
| | $\Delta H_{rxn}$ | −12.2 | −15.4 | −10.7 | 0.0 | 0.0 | 0.0 | −39.7 | −26.2 | −24.2 | −16.5 | −7.2 |
| B3LYP/6-31G* | $\Delta H^{\ddagger}$ | 33.9 (35.6) | 30.1 (30.2) | 27.3 (27.9) | 36.6 (38.7)[85,96] 36.5[8,96] 36.6[85,87] | 26.6 (28.9) 27.0[87] | 34.1 (34.4)[80] 34.2[81] [33.2][80] | 24.9[9g',81,82,97] (22.4)[9q,83,82] 24.8[9t,98] 22.7[89] | 22.2 (19.9) 22.4[9h',9z] (19.0)[84] [21.1][99] | 21.1 (19.3) (19.4)[99] [21.0][99] | 22.0[100,101] (23.7) | 50.4[100,101] (53.9) |
| | $\Delta S^{\ddagger}$ | 0.0 | −5.6 | −2.8 | −6.7 | −1.2 | −8.7 | −42.8 | −42.1 | −45.7 | 1.5 | 5.3 |
| | $\Delta H_{rxn}$ | −12.7 | −12.5 | −14.1 | 0.0 | 0.0 | 0.0 | −36.6[9t] | −18.6 | −11.1 | −20.8 | −13.9[100,101] |
| | $\Delta S_{rxn}$ | 2.2 | −7.4 | −4.3 | 0.0 | 0.0 | 0.0 | −44.6 | −46.1 | −50.8 | 5.4 | 12.1 |
| B3LYP/6-31+G** | $\Delta H^{\ddagger}$ | 32.1 | 30.7 | 26.9 | 35.7 | 25.5 | 34.1 | 27.2 | 24.7 | 23.2 | 20.8 | 48.4 |
| | $\Delta S^{\ddagger}$ | 0.0 | −5.7 | −3.7 | −6.8 | −1.2 | −8.3 | −42.7 | −42.4 | −45.9 | 1.6 | 5.2 |
| | $\Delta H_{rxn}$ | −14.7 | −10.6 | −12.2 | 0.0 | 0.0 | 0.0 | −31.3 | −13.5 | −6.1 | −22.9 | −18.3 |
| | $\Delta S_{rxn}$ | 2.2 | −7.6 | −5.2 | 0.0 | 0.0 | 0.0 | −45.9 | −46.0 | −50.8 | 4.1 | 11.9 |
| B3LYP/6-311+G(2d,p)[b] | $\Delta H^{\ddagger}$ | 31.4 | 30.8 | 24.4 | 36.2 | 25.5 | 34.9 | 26.2 | 26.0 | 25.2 | 19.2 | 46.0 |
| | $\Delta H_{rxn}$ | −14.0 | −9.8 | −13.8 | 0.0 | 0.0 | 0.0 | −30.9 | −11.0 | −3.8 | −26.4 | −22.0 |
| BPW91/6-31G* | $\Delta H^{\ddagger}$ | 32.2 | 26.2 | 22.8 | 30.3 | 23.3 | 27.6 (27.6)[80] [26.7][80] | 19.9 | 17.6 | 16.4 | 19.0 | 45.9 |
| | $\Delta S^{\ddagger}$ | 0.0 | −5.6 | −4.0 | −7.0 | −1.2 | −9.2 | −41.2 | −41.5 | −43.9 | 1.7 | 5.8 |
| | $\Delta H_{rxn}$ | −9.8 | −12.4 | −16.1 | 0.0 | 0.0 | 0.0 | −38.2 | −20.8 | −12.3 | −13.3 | −5.9 |
| | $\Delta S_{rxn}$ | 2.2 | −7.5 | −5.5 | 0.0 | 0.0 | 0.0 | −47.3 | −45.9 | −50.7 | 5.7 | 12.4 |
| MPW1K/6-31+G** | $\Delta H^{\ddagger}$ | 38.7 | 30.4 | 27.2 | 37.7 | 24.9 | 36.7 | 24.4 | 20.6 | 19.2 | 32.2 | 65.1 |
| | $\Delta S^{\ddagger}$ | 1.3 | −5.6 | −3.5 | −8.4 | −1.4 | −9.1 | −42.2 | −42.2 | −46.0 | 1.5 | 4.5 |
| | $\Delta H_{rxn}$ | −7.7 | −19.7 | −20.5 | 0.0 | 0.0 | 0.0 | −48.4 | −30.3 | −23.7 | −6.6 | 1.9 |
| | $\Delta S_{rxn}$ | 3.6 | −7.8 | −5.0 | 0.0 | 0.0 | 0.0 | −46.1 | −43.1 | −51.1 | 5.5 | 11.9 |
| KMLYP/6-31G* | $\Delta H^{\ddagger}$ | 42.2 | 31.5 | 29.6 | 39.2 | 27.2 | 38.4 | 21.1 | 17.2 | 15.1 | 36.8 | 71.9 |
| | $\Delta S^{\ddagger}$ | −1.5 | −3.6 | −3.7 | −6.7 | 0.2 | −9.2 | −41.2 | −41.9 | −44.8 | 1.5 | 4.2 |
| | $\Delta H_{rxn}$ | −5.8 | −23.7 | −22.6 | 0.0 | 0.0 | 0.0 | −59.4 | −39.8 | −33.8 | −4.7 | −6.0 |
| | $\Delta S_{rxn}$ | 2.2 | −7.4 | −3.7 | 0.0 | 0.0 | 0.0 | −46.1 | −46.0 | −51.1 | 7.4 | 12.2 |
| KMLYP/6-311G | $\Delta H^{\ddagger}$ | 38.0 | 32.1 | 30.9 | 39.3 | 30.2 | 38.4 | 22.4 | 19.1 | 16.5 | 31.8 | 64.6 |
| | $\Delta S^{\ddagger}$ | +1.2 | −8.8 | −3.7 | −6.9 | −1.1 | −9.1 | 42.7 | −42.5 | −46.2 | 3.7 | 4.5 |
| | $\Delta H_{rxn}$ | −0.4 | −19.9 | −17.2 | 0.0 | 0.0 | 0.0 | −51.4 | −32.8 | −28.5 | −17.8 | −5.6 |
| | $\Delta S_{rxn}$ | 3.6 | −8.8 | −5.1 | 0.0 | 0.0 | 0.0 | −46.1 | −46.0 | −51.1 | 7.4 | 12.2 |
| CBS-QB3 | $\Delta H^{\ddagger}$ | 32.0 | 28.8 | 25.2 | 36.8 | 25.8 | 33.0 | 22.9 | 17.3 | 11.6 | 21.5 | |
| | $\Delta S^{\ddagger}$ | −1.4 | −4.1 | −3.6 | −6.8 | 0.2 | −7.9 | −40.6 | −40.7 | −44.5 | 1.9 | |
| | $\Delta H_{rxn}$ | −12.6 | −14.8 | −12.8 | 0.0 | 0.0 | 0.0 | −38.3 | −24.6 | −22.2 | −19.8 | |

[a] Energies are given for without zero-point correction (parentheses) and with ZPE and thermal corrections for 298 K [square bracket] and 500 K [[double bracket]]. All values are given in kcal/mol. [b] Single-point calculation with B3LYP/6-31+G**-optimized geometry.
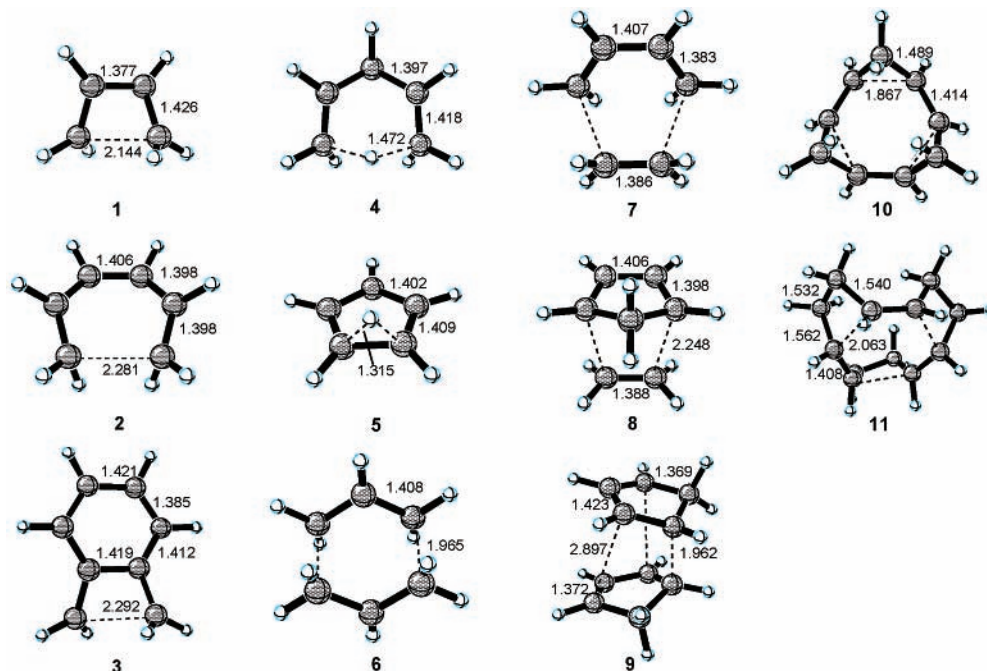
**Figure 2.** B3LYP/6-31G* geometries of transition structures for pericyclic reactions 1−11. Bond lengths are in angstroms.

**TABLE 4: Mean Deviations (MD), Mean Absolute Deviations (MAD), Standard Deviations (SD), and Maximum Negative and Positive Errors of Predicted $\Delta H^{\ddagger}_{0K}$ Relative to Experimental Values for Reactions 1−9[a]**

|  | MD | MAD | SD | max (−) error | max (+) error |
|---|---|---|---|---|---|
| B3LYP/6-31G* | +1.2 | 1.7 | 1.9 | 1.9[e] | 6.0[i] |
| CBS-QB3 | −1.4 | 1.9 | 1.6 | 4.3[h] | 2.1[f] |
| MPW1K/6-31+G** | +1.5 | 2.2 | 2.1 | 2.0[e] | 6.9[d] |
| B3LYP/6-31+G** | +1.5 | 2.4 | 2.5 | 2.3[e] | 8.1[i] |
| CASPT2/6-31G*//CASSCF | +0.3 | 2.4 | 1.6 | 3.8[e] | 5.7[f] |
| CASPT2/6-31G*//B3LYP | −0.1 | 2.8 | 1.8 | 4.5[e] | 5.1[f] |
| B3LYP/6-311+G(2d,p)[b] | +1.6 | 2.9 | 3.2 | 4.8[e] | 10.1[i] |
| KMLYP/6-311G | +2.3 | 3.1 | 2.0 | 2.5[h] | 6.5[d] |
| KMLYP/6-31G* | +1.7 | 3.2 | 3.1 | 4.4[h] | 10.3[d] |
| BPW91/6-31G* | −3.3 | 3.7 | 2.6 | 6.9[g] | 1.3[i] |
| MP2/6-31G* | −3.0 | 4.6 | 2.3 | 7.6[i] | 3.9[d] |
| CASSCF/6-31G* | +16.0 | 16.0 | 9.7 | c | 34.6[i] |
| HF/6-31G* | +18.7 | 18.7 | 5.4 | c | 26.7[i] |

[a] All quantities are in kcal/mol. [b] Single point calculation on the B3LYP/6-31+G** optimized geometry. [c] None of the activation enthalpies calculated with HF or CASSCF are lower than the experimental value. [d] Ring opening of cyclobutene to butadiene. [e] Ring closing of *o*-xylylene to benzocyclobutane. [f] 1,5-H shift of cyclopentadiene. [g] Cope rearrangement of 1,5-hexadiene. [h] Diels−Alder reaction between cyclopentadiene and ethylene. [i] Dimerization of cyclopentadiene.

## Comparisons of Experimental and Computed Activation Enthalpies

As noted earlier, the experimental activation energies for reactions 10 and 11 are rather rough estimates; therefore, we deleted these from our test set for the statistical analysis of the computed activation enthalpies. Table 4 lists the mean deviation (MD), mean absolute deviation (MAD), standard deviation (SD) of the mean absolute deviations, and the largest positive and negative errors for the computed 0 K activation enthalpies from the experimental values for the set of 11 reactions. Deviations of calculated activation enthalpies from experimental values by each method are depicted graphically in Figure 3. The mean absolute deviation (◆) shows the types of errors that are typical,

**TABLE 5: OLYP and O3LYP Activation Enthalpies[23] [a]**

|  | $\Delta H^{\ddagger}$ (kcal/mol) | |
|---|---|---|
|  | Reaction 1 | Reaction 7 |
| Experimental | 31.9±0.2 | 23.3±2 |
| CBS-QB3 | 32.0 | 22.9 |
| B3LYP/6-31G* | 33.9 | 24.9 |
| OLYP/6-31G* | 33.8 | 25.2 |
| OLYP/6-311G(*2df,2pd*) | 32.4 | 27.7 |
| O3LYP/6-31G* | 35.6 | 25.4 |
| O3LYP/6-311G(*2df,2pd*) | 34.1 | 27.9 |

[a] Experimental, CBS-QB3, and B3LYP/6-31G* results are given for comparison.

the standard deviation (error bars) shows the spread of the error from the mean, and the green box gives the worst absolute errors.

The first five methods plotted in Figure 3 all give very good results on average (MAD < 2.5 kcal/mol), and because of the small number of reactions involved in our reaction set, there is little, if any, statistical difference in performance. B3LYP/6-31G* does have the smallest mean absolute deviation, while the high-accuracy CBS-QB3 and CASPT2 methods are also in this first class, having notably smaller maximum absolute errors than the DFT methods. Both BPW91 and MP2 have somewhat higher MADs, although the SD is quite good. HF and CASSCF give large positive errors and MADs due to the systematic neglect of correlation energy (HF) or correlation involving the nonactive space (CASSCF). Because correlation energy is larger for transition structures than for reactants, the activation enthalpies are much too high.

Figures 4−6 compare how well the various methods were able to predict specific activation enthalpies. Figure 4a compares the methods that had the lowest MADs. In general, CBS-QB3 and CASPT2/6-31G*//CASSCF/6-31G* show very good agreement with each other and with experiment. The largest deviations from experiment are observed for reactions 3, 5, 8, 9, and
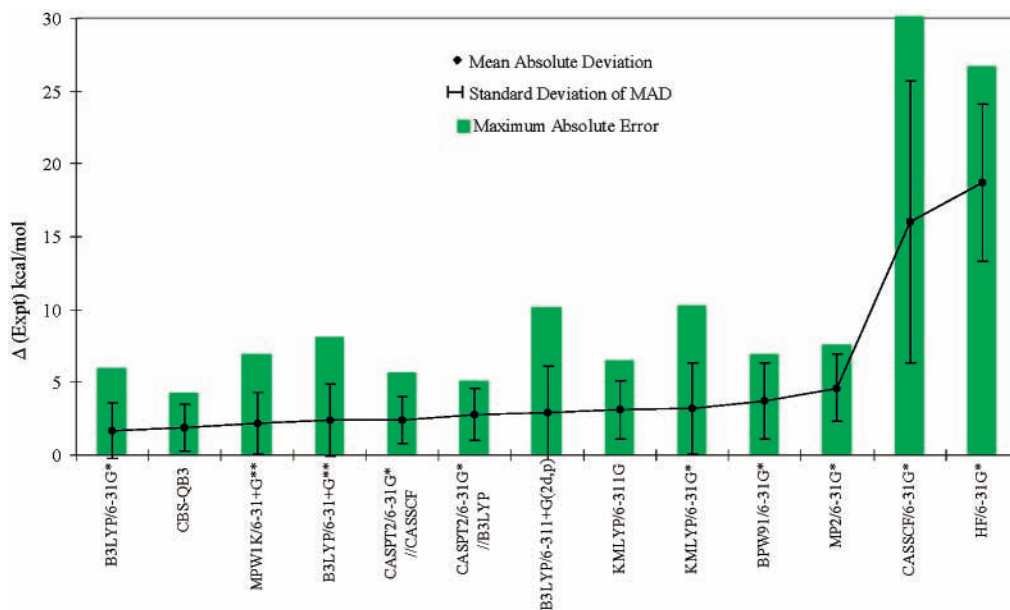
**Figure 3.** Statistical assessment of performance of different methods for the prediction of $\Delta H^{\ddagger}_{0K}$ for pericyclic reactions 1−9.
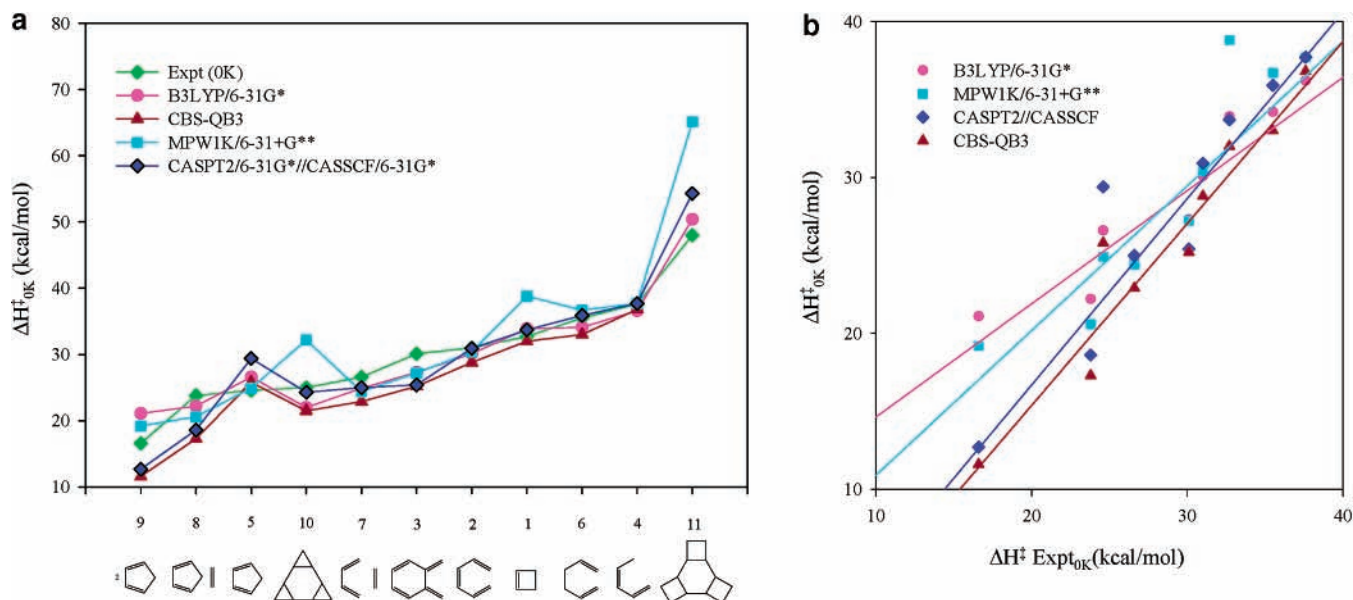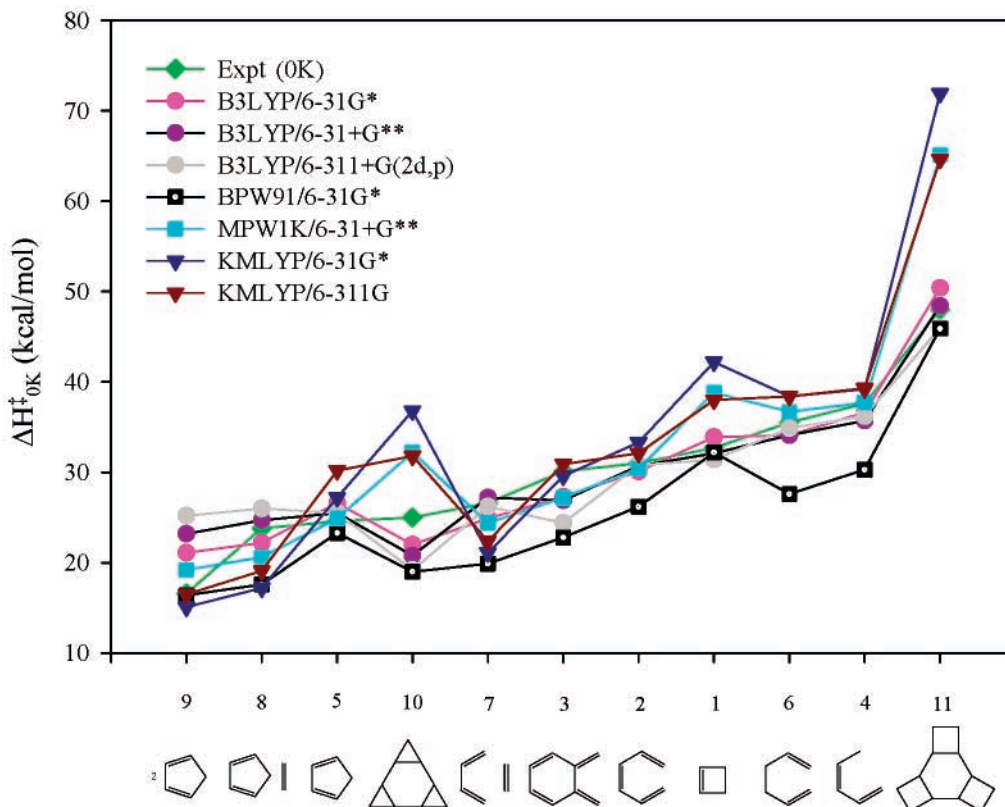


**Figure 4.** (a) Comparisons of experimental activation enthalpies for 11 pericyclic reactions to predictions by 4 methods with the lowest mean absolute deviations. The data are arranged in order of increasing experimental activation enthalpies. (b) Plot of computed activation enthalpies vs experimental activation enthalpies for reactions 1−9. The linear regressions obtained are shown. B3LYP/6-31G*: $n = 9$, $y = 0.726x + 7.367$, $R^2 = 0.860$. MPW1K: $n = 9$, $y = 0.928x + 1.620$, $R^2 = 0.834$. CASPT2: $n = 9$, $y = 1.196x − 7.240$, $R^2 = 0.914$. CBS-QB3: $n = 9$, $y = 1.167x − 7.972$, $R^2 = 0.944$.

11. B3LYP/6-31G* shows good agreement with experiment but shows large deviations from CBS-QB3 and CASPT2//CASSCF for reaction 8 and especially reaction 9. A preliminary inquiry into this observation suggests that B3LYP incorrectly predicts the strain of the norbornene framework leading to systematic errors in the calculation of activation enthalpies (and reaction enthalpies) involving this moiety.[102] MPW1K performs well for most reaction barriers with reactions 10 and 11 being the exceptions. Inclusion of 10 and 11 in the statistical analyses would have resulted in a significantly higher MAD for MPW1K. Figure 4b is a plot of the computational activation enthalpies vs experimental values to show the different trends of the most accurate methods. CASPT2//CASSCF and CBS-QB3 perform best by the criterion of $R^2$ values.

Figure 5 compares the behavior of all of the DFT methods to the experimentally determined activation enthalpies. Several

trends are found. BPW91/6-31G* systematically underestimates the activation enthalpies. On the other extreme, KMLYP tends to overestimate the activation enthalpies. Of the two basis sets used with KMLYP, the 6-311G gives better results than the 6-31G* basis set. Musgrave has found that better results are obtained by pairing this functional with much larger basis sets; errors are reduced by as much as 2−3 kcal/mol.[103] Both B3LYP/6-31G* and 6-31+G** perform quite well, but B3LYP with the 6-311+G(2d,p) basis set shows larger deviations and errors compared to the smaller basis sets used in this study for these hydrocarbon reactions. B3LYP gives good results even with the relatively small 6-31G* basis set.

Figure 6 illustrates the expected systematic overestimation of the activation enthalpies by HF and CASSCF methods. This is understood, since HF neglects correlation energy and CASSCF only includes correlation between the electrons in the

**Figure 5.** Comparisons of experimental activation enthalpies for 11 pericyclic reactions to predictions by DFT methods. The data are arranged in order of increasing experimental activation enthalpies.
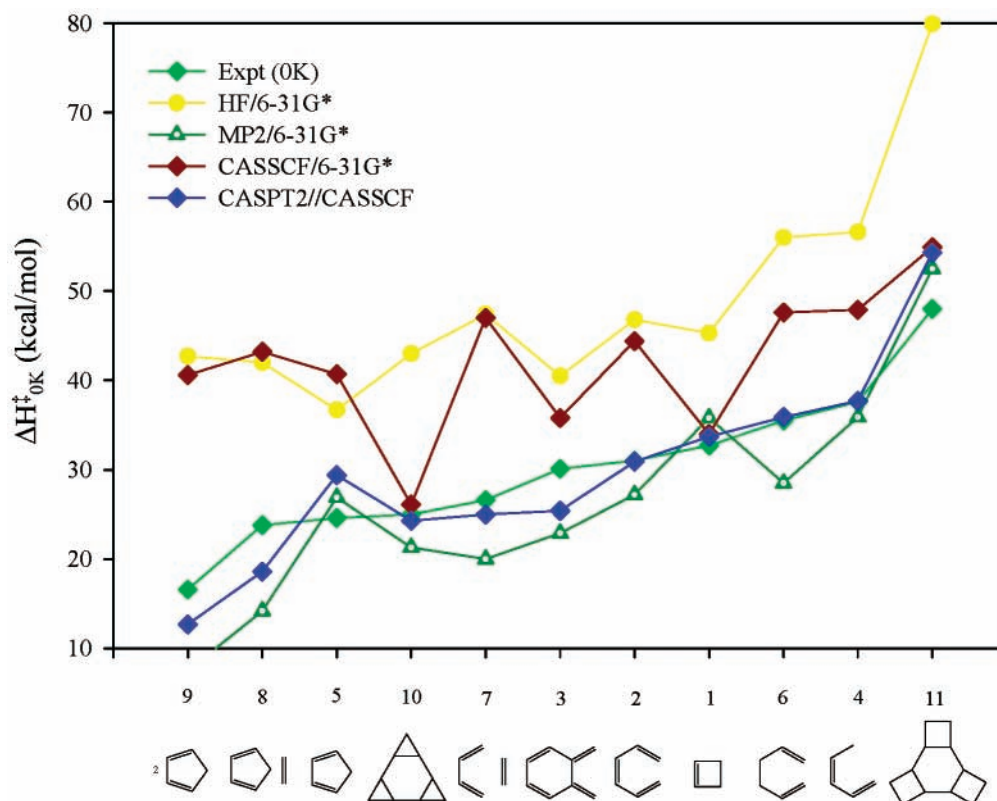


**Figure 6.** Comparisons of experimental activation enthalpies for 11 pericyclic reactions to prediction methods having known systematic errors in the calculation of activation enthalpies. The data are arranged in order of increasing experimental activation enthalpies.

active space. The MP2 method overcorrects for the lack of correlation energy in an HF calculation and tends to predict barriers that are lower than experiment. CASPT2 single points on CASSCF geometries are an accurate way of recovering

nondynamical correlation energy and predicting highly accurate activation enthalpies.

Pulay and Baker[23] have tested the performance of OLYP and O3LYP with the 6-31G* and 6-311G(2df,2pd) basis sets for
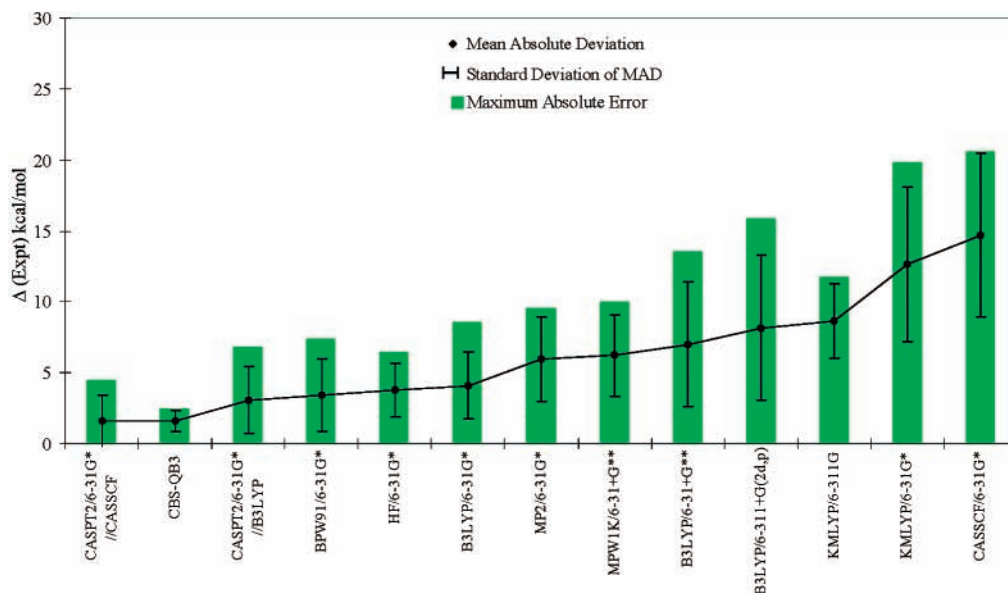
**Figure 7.** Statistical assessment of the performance of different methods for the prediction of $\Delta H_{rxn,0K}$ for six pericyclic reactions. Differences are given in kcal/mol, with the computed values subtracted from the experimental values.

**TABLE 6: Mean Deviations (MD), Mean Absolute Deviations (MAD), Standard Deviations (SD), and Maximum Negative and Positive Errors Relative to Experiment for Six Calculated Energies of Reaction (kcal/mol)**

|  | MD | MAD | SD | max (−) error | max (+) error |
|---|---|---|---|---|---|
| CASPT2/6-31G*//CASSCF | −1.6 | 1.6 | 1.8 | 4.5[g] | b |
| CBS-QB3 | −1.0 | 1.6 | 0.7 | 2.5[g] | 1.3[e] |
| CASPT2/6-31G*//B3LYP | −3.1 | 3.1 | 2.3 | 6.8[g] | b |
| BPW91/6-31G* | +1.6 | 3.4 | 2.5 | 5.6[d] | 7.4[g] |
| HF/6-31G* | +1.4 | 3.8 | 1.9 | 4.4[d] | 6.5[g] |
| B3LYP/6-31G* | +2.2 | 4.1 | 2.4 | 3.6[d] | 8.6[g] |
| MP2/6-31G* | −5.4 | 6.0 | 3.0 | 9.6[d] | 1.6[c] |
| MPW1K/6-31+G** | −5.2 | 6.2 | 2.8 | 10.0[d] | 3.0[c] |
| B3LYP/6-31+G** | +5.1 | 7.0 | 4.4 | 4.0[c] | 13.6[g] |
| B3LYP/6-311+G(2d,p)[a] | +5.9 | 8.2 | 5.1 | 3.3[c,d] | 5.9[f] |
| KMLYP/6-311G | −5.2 | 8.6 | 2.6 | 11.8[e] | b |
| KMLYP/6-31G* | −11.0 | 12.7 | 5.4 | 19.8[e] | 4.9[c] |
| CASSCF/6-31G* | +11.5 | 14.7 | 5.8 | 9.7[c] | 20.6[e] |

[a] Single-point calculation on the B3LYP/6-31+G**-optimized geometry. [b] None of the calculated energies of reaction were less exothermic than the experimental values. [c] Ring opening of cyclobutene to butadiene. [d] Ring opening of *o*-xylylene to benzocyclobutane. [e] Diels−Alder reaction between butadiene and ethylene. [f] Diels−Alder reaction between cyclopentadiene and ethylene. [g] Dimerization of cyclopentadiene.

the calculation of two reactions studied here. Both reaction 1 (the cycloreversion of cyclobutene) and reaction 7 (the Diels−Alder of butadiene plus ethylene) were explored.[23] Table 5 compares their results with the experimental data, the CBS-QB3 results, and the best DFT method studied here, B3LYP/6-31G*. In general, the OLYP/6-31G* activation enthalpies are very similar to those calculated using B3LYP/6-31G*. For the two reported reactions, the OLYP/6-311G(2df,2pd) method gives activation enthalpies closest to experiment, while O3LYP overestimates the barriers.

**Comparison of Experimental and Computed Reaction Enthalpies**

Table 6 lists the MD, MAD, SD, and the largest positive and negative errors for the computed 0 K enthalpies of reaction from the experimental values for the set of six reactions. Deviations of calculated reaction enthalpies from experimental values by

each method are depicted graphically in Figure 7. Only six reaction enthalpies are available, so the results do not have much statistical significance.

Similar to the trends observed for the computed activation enthalpies, the first six methods plotted in Figure 7 tend to give accurate results and perform significantly better than the remaining methods. While CASPT2/6-31G*//CASSCF/6-31G* and CBS-QB3 have the lowest MADs, CBS-QB3 stands out as the method that provides the greatest reliability, having a standard deviation of the MAD of only 0.7 kcal/mol. BPW91 and B3LYP/6-31G* perform the best of the DFT methods. Although the HF method systematically overestimates activation enthalpies, it is one of the best methods for calculating reaction enthalpies.

**Evaluation of Experimental Enthalpies of Activation**

As depicted in Figure 4a, most reactions show small variations between the activation enthalpies determined by the most reliable theoretical methods and the experimental data. Several reactions, however, show significant disagreement between theory and experiment; these reactions are 9 (Diels−Alder dimerization of cyclopentadiene), 3 (electrocyclization of *o*-xylylene), and 10 (cycloreversion of *cis*-triscyclopropacyclohexane). Each of these cases will be discussed.

The calculated activation enthalpies for reaction 9 range from 11.6 kcal/mol (CBS-QB3) to 23.2 kcal/mol (B3LYP/6-31+G**), while the best experimental measurement is taken as 16.6 kcal/mol. Particularly disturbing is the disagreement of B3LYP (which overestimates the barrier by +6.6 and +4.5 kcal/mol) with CASPT2//CASSCF and CBS-QB3 (which underestimate the barrier by −3.9 and −5.0 kcal/mol). Because it is suspected that B3LYP has systematic error in the calculation of the norbornene structure,[102] the CASPT2//CASSCF and CBS-QB3 activation enthalpies are taken as the most reliable (12.7 and 11.6 kcal/mol, respectively). An average of these two values suggests that the experimental activation enthalpy may be closer to 12.2 kcal/mol. This value is in close agreement with the gas-phase barrier reported by Kistiakowsky and Mears.[54]

In reaction 3, activation parameters are obtained from dimerization rate of *o*-xylylene (**1**) which is formed by flash photolysis of 5,6-dimethylbicyclo[2.2.1]hept-2-ene-7-one and

**TABLE 7: Mean Deviations (MD), Mean Absolute Deviations (MAD), Standard Devations (SD) of the MAD, and Maximum Negative and Positive Errors Relative to CBS-QB3 Calculated Enthalpies of Activation[a]**

|  | MD | MAD | SD | max (−) error | max (+) error |
|---|---|---|---|---|---|
| CASPT2/6-31G*//B3LYP | +1.5 | 1.6 | 1.6 | 0.5[f] | 4.5[j] |
| CASPT2/6-31G*//CASSCF | +1.7 | 1.7 | 1.1 | c | 3.6[h] |
| MP2/6-31G* | −1.3 | 2.2 | 1.6 | 4.4[i] | 3.8[e] |
| B3LYP/6-31G* | +2.4 | 2.2 | 2.8 | 0.2[g] | 9.5[k] |
| BPW91/6-31G* | −1.8 | 2.7 | 2.1 | 6.5[g] | d |
| B3LYP/6-31+G** | +2.4 | 2.7 | 3.7 | 1.1[g] | 11.6[k] |
| B3LYP/6-311+G(2d,p)[b] | +2.3 | 3.1 | 4.2 | 2.3[l] | 13.6[k] |
| MPW1K/6-31+G** | +3.4 | 3.5 | 3.4 | 0.9[h] | 10.7[l] |
| KMLYP/6-311G | +4.0 | 4.1 | 2.9 | 0.5[j] | 10.3[l] |
| KMLYP/6-31G* | +3.9 | 4.3 | 4.7 | −1.8[j] | 15.3[l] |
| CASSCF/6-31G* | +14.0 | 14.0 | 9.9 | c | 31.1[k] |
| HF/6-31G* | +18.3 | 18.3 | 8.3 | c | 30.5[k] |

[a] All quantities are in kcal/mol. [b] Single-point calculation on the B3LYP/6-31+G**-optimized geometry. [c] None of the activation enthalpies calculated with HF or CASSCF are lower than the CBS-QB3 value. [d] None of the activation enthalpies calculated with BPW91 are higher than the CBS-QB3 value. [e] Ring opening of cyclobutene to butadiene. [f] Ring closing of *o*-xylylene to benzocyclobutane. [g] 1,5-H shift in 1,3-pentadiene. [h] 1,5-H shift of cyclopentadiene. [i] Cope rearrangement of 1,5-hexadiene. [j] Diels−Alder reaction between butadiene and ethylene. [k] Dimerization of cyclopentadiene. [l] Ring opening of *cis*-tris-cyclopropacyclohexane.

thermolysis of benzocyclobutene. B3LYP/6-31G*, B3LYP/6-31+G**, CBS-QB3, and CASPT2//CASSCF predict activation enthalpies of 27.3, 26.9, 25.2, and 25.4 kcal/mol and are in close agreement with each other. However, all four methods predict barriers that are 2−4 kcal/mol lower than experimental value (30.1 kcal/mol), suggesting that a value of 25 kcal/mol is more reasonable for this barrier.
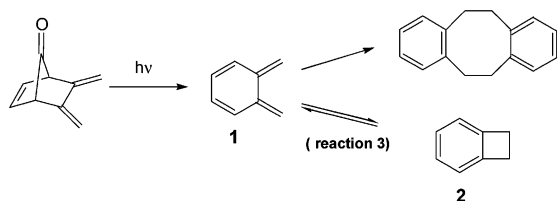


In the cycloreversion of *cis*-triscyclopropacyclohexane (reaction 10), CASPT2/6-31G*//CASSCF is the only one of the most reliable methods to give good agreement (24.3 kcal/mol) with the experimental estimate of 24.4 kcal/mol. Both B3LYP and CBS-QB3 predict that the activation enthalpy is ~2 kcal/mol lower than the reported experimental range. Because the experimental activation enthalpy for reaction 10 involved rather large presumptions and may have errors of ±3 kcal/mol, it is likely that the true experimental barrier for reaction 10 is lower than the reported value. An average of the B3LYP/6-31G*, CBS-QB3, and the CASPT2//CASSCF calculated barriers suggests that a more accurate estimate of the activation enthalpy would be ~23 kcal/mol.

There are also differences between computed and experimental activation barriers for reaction 11, but the experimental value is only a rough estimate, and CBS-QB3 predictions are unavailable since the molecules have twelve heavy atoms, too large for the CCSD(T) and CBS extrapolation steps to be completed on any accessible computer.
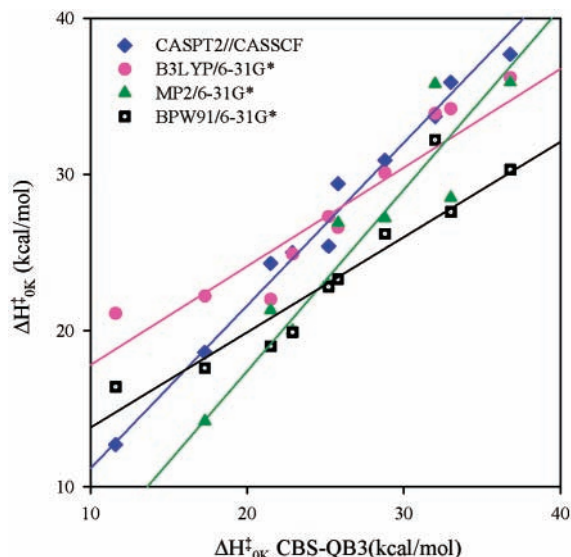


**Figure 8.** Plot of computed activation enthalpies vs CBS-QB3 activation enthalpies. The linear regression is plotted for each method. CASPT2: $n = 10$, $y = 1.042x + 0.751$, $R^2 = 0.990$. B3LYP: $n = 10$, $y = 0.632x + 11.483$, $R^2 = 0.867$. MP2: $n = 10$, $y = 1.162x - 5.831$, $R^2 = 0.977$. BPW91: $n = 10$, $y = 0.610x + 7.695$, $R^2 = 0.882$.

## Comparison of Computed Values with CBS-QB3 Computed Values

The statistical analysis presented above is only as useful as the accuracy of the experimental standard. Because of the revision of three of the experimental activation enthalpies, the accuracies of the various computational methods were reanalyzed. However, for this analysis, we have taken the CBS-QB3 activation enthalpies and reaction enthalpies as the standard for the comparison in place of the experimental values, on the presumption that the accuracy of the CBS-QB3 calculations is highest.

Table 7 lists the MDs, MADs, standard deviations of the MAD, and maximum errors for the computed activation enthalpies relative to the CBS-QB3 computed activation enthalpies. In general, the MADs for all methods are smaller when compared to CBS-QB3 than when compared to experiment. As before, CASPT2//CASSCF and B3LYP/6-31G* perform very well. The most significant change occurs for MP2/6-31G(d), which has an MAD of 5.3 kcal/mol when compared to experiment and an MAD of only 2.2 kcal/mol when compared to CBS-QB3. B3LYP/6-31G* fares worse, but this is primarily due to the significant deviation from experiment for one reaction, the dimerization of cyclopentadiene. Figure 8 is the same as 4b, but compares CASPT2//CASSCF, B3LYP/6-31G*, MP2/6-31G*, and BPW91/6-31G* to CBS-QB3.

Table 8 lists the MDs, MADs, standard deviations of the MAD, and maximum errors for the computed reaction enthalpies relative to the CBS-QB3 reaction enthalpies. In the case of reaction enthalpies, comparisons to experiment and to CBS-QB3 are very similar, as reflected in the very small changes in the MADs. As before, CASPT2//CASSCF, BPW91, B3LYP/6-31G*, and HF perform the best of the methods tested here.

## Comparisons of Computed Transition Structure Geometries

B3LYP has proven reliable in reproducing experimental kinetic isotope effects.[11] This indicates that B3LYP/6-31G* provides excellent geometries for reactants, products, and transition structures. We have compared the partial bond lengths

Benchmarking Computational Methods

*J. Phys. Chem. A, Vol. 107, No. 51, 2003* **11457**

**TABLE 8: Mean Deviations (MD), Mean Absolute Deviations (MAD), Standard Deviations (SD), Maximum Negative and Positive Errors Relative to CBS-QB3 for Six Calculated Energies of Reaction (kcal/mol)**

| | MD | MAD | SD | max (−) error | max (+) error |
|---|---|---|---|---|---|
| HF/6-31G* | +2.4 | 3.4 | 3.4 | 2.1[d] | 9.0[g] |
| MP2/6-31G* | −4.4 | 5.5 | 1.7 | 7.6[e] | 3.5[c] |
| CASSCF/6-31G* | +12.5 | 15.1 | 6.5 | 7.8[c] | 21.7[f] |
| CASPT2/6-31G*//B3LYP | −2.0 | 2.5 | 1.4 | 4.3[g] | [b] |
| CASPT2/6-31G*//CASSCF | −0.5 | 1.4 | 0.7 | 2.0[g] | [b] |
| B3LYP/6-31G* | +3.3 | 3.8 | 4.1 | 1.3[d] | 11.1[g] |
| B3LYP/6-31+G** | +6.2 | 6.9 | 5.9 | 2.1[c] | 16.1[g] |
| B3LYP/6-311+G(2d,p)[a] | +7.0 | 7.8 | 6.9 | 1.4[c] | 18.4[g] |
| BPW91/6-31G* | +2.6 | 3.7 | 3.3 | 3.3[d] | 9.9[g] |
| MPW1K/6-31+G** | −4.2 | 5.8 | 2.9 | 10.1[e] | 4.9[c] |
| KMLYP/6-31G* | −9.9 | 12.2 | 5.2 | 21.1[e] | 6.8[c] |
| KMLYP/6-311G | −4.2 | 8.2 | 3.7 | 13.1[e] | [b] |

[a] Single-point calculation on the B3LYP/6-31+G**-optimized geometry. [b] None of the calculated energies of reaction were less exothermic than the calculated CBS-QB3 values. [c] Ring opening of cyclobutene to butadiene. [d] Ring opening of *o*-xylylene to benzocyclobutane. [e] Diels−Alder reaction between butadiene and ethylene. [f] Diels−Alder reaction between cyclopentadiene and ethylene. [g] Dimerization of cyclopentadiene.
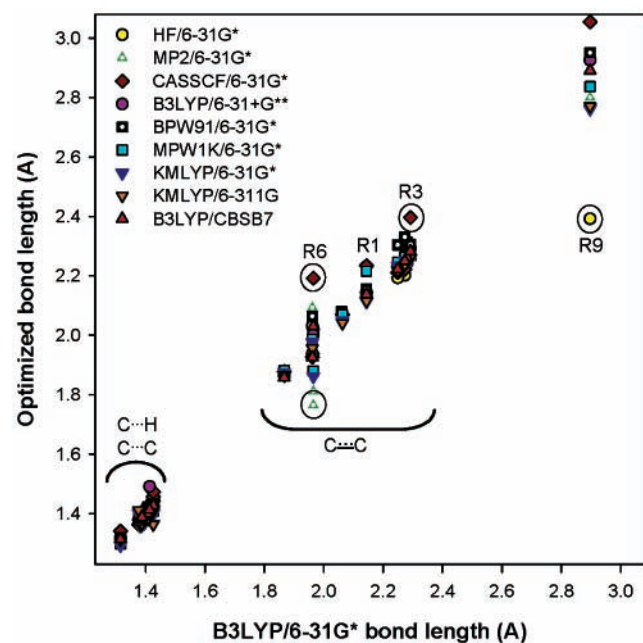


**Figure 9.** Partial bond lengths calculated with various methods plotted vs B3LYP/6-31G* values. Geometric parameters that deviate significantly from B3LYP/6-31G* are identified by reaction.

of the calculated transition structures predicted by HF/6-31G*, B3LYP/6-31+G**, BPW91/6-31G*, MPW1K/6-31+G**, CBS-QB3 (which employs a B3LYP/CBSB7(5D,7F) geometry optimization), KMLYP/6-31G*, KMLYP/6-311G, and CASSCF/6-31G* to those partial bond lengths predicted by B3LYP/6-31G* (Figure 9).

In Figure 9, three types of partial bonds lengths are observed: (1) partial single CC bonds from 1.8 to 2.4 Å, (2) partial double CC bonds from 1.3 to 1.5 Å, and (3) partial CH bonds from 1.3 to 1.4 Å. One exceptional bond type is also observed in reaction 9, the dimerization of cyclopentadiene, due to the bispericyclic nature of the transition structure.[99] This CC bond distance ranges from 2.4 to 3.1 Å. In general, there is very good agreement of bond lengths predicted by the various methods, with the following exceptions.

**TABLE 9: Summary of the Recommended $\Delta H^{\ddagger}_{0K}$ and $\Delta H_{rxn,0K}$ Values for Hydrocarbon Pericyclic Reactions 1−11[a]**

| reaction | $\Delta H^{\ddagger}_{0K}$ (kcal/mol) | $\Delta H_{rxn,0K}$ (kcal/mol) |
|---|---|---|
| 1 | 31.9 ± 0.2 | −10.6 ± 1 |
| 2 | 30.2 ± 0.5 | −15.3 ± 1 |
| 3 | 25 ± 2[b] | −10.5 ± 1 |
| 4 | 36.7 ± 0.5 | 0.0 |
| 5 | 23.7 ± 0.5 | 0.0 |
| 6 | 34.5 ± 0.5 | 0.0 |
| 7 | 23.3 ± 2 | −39.6 ± 1 |
| 8 | 21.6 ± 1.6 | −23.2 ± 0.6 |
| 9 | 12 ± 2[b] | −19.7 (g) |
| 10 | 23 ± 3[b] | −18 ± 2[c] |
| 11 | 46.5 ± 3 | −6 ± 2[d] |

[a] Unless otherwise noted, these values are taken from Table 1. [b] Experimental data are revised based on the computational results. See above discussion. [c] Estimate is based on an average of CASPT2// CASSCF and CBS-QB3 computational results. No experimental data are available. [d] Estimate is based on an average of CASPT2//B3LYP and CASPT2//CASSCF computational results. No experimental data are available.

In the dimerization of cyclopentadiene (reaction 9), all but one method give highly asynchronous transition structures which are bispericyclic, corresponding simultaneously to [4 + 2] and [2 + 4] reactivity; only HF gives a transition structure that is nearly synchronous and shows pure [4 + 2] reactivity. In the Cope rearrangement (reaction 6), the $C_{2h}$ symmetry of the transition structure obtained by most methods was disturbed when the MP2 optimization was carried out because a stepwise process is predicted by this method.[80]
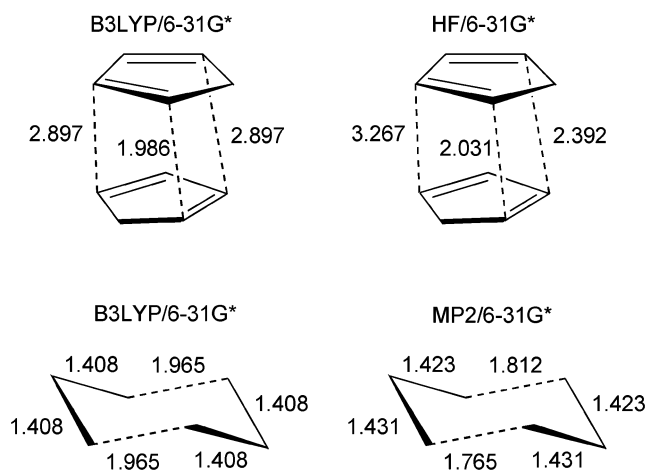


**Conclusions**

The experimental activation barriers of 11 pericyclic reactions have been evaluated and compared to predictions by a variety of methods. The performance of the relatively computationally inexpensive DFT method, B3LYP/6-31G*, compares well with the higher-accuracy but more expensive CASPT2 and CBS-QB3 methods. Other density functionals also perform well for these hydrocarbon pericyclic processes, although larger basis sets are needed to achieve comparable accuracy.

Recommended values for the $\Delta H^{\ddagger}_{0K}$ and $\Delta H_{rxn,0K}$ for reactions 1−11 are given in Table 9. These will be of use for the benchmarking of other methods. Also, additional pericyclic processes will be assessed in order to increase the statistical significance of these benchmarks.

Guner et al.

### References and Notes

(1) Understanding Chemical Reactivity. In *Quantum-Mechanical Prediction of Thermochemical Data*; Cioslowski, J., Ed.; Kluwer Academic Publishers: Boston, MA, 2001; Vol. 22, pp 1−245.

(2) (a) Curtiss, L. A.; Raghavachari, K.; Redfern, P. C.; Pople, J. A. *J. Chem. Phys.* **2000**, *112*, 1125−1132. (b) Curtiss, L. A.; Raghavachari, K.; Redfern, P. C.; Pople, J. A. *J. Chem. Phys.* **2000**, *112*, 7374−7383. (c) Curtiss, L. A.; Redfern, P. C.; Raghavachari, K.; Pople, J. A. *J. Chem. Phys.* **2001**, *114*, 108−117. (d) Redfern, P. C.; Zapol, P.; Curtiss, L. A.; Raghavachari, K. *J. Phys. Chem. A* **2000**, *104*, 5850−5854. (e) Curtiss, L. A.; Raghavachari, K.; Trucks, G. W. *J. Phys. Chem. A* **1991**, *94*, 7221. (f) Curtiss, L. A.; Raghavachari, K. *Theor. Chem. Acc.* **2002**, *108*, 61−70.

(3) Henry, D. J.; Parkinson, C. J.; Mayer, P. M.; Radom, L. *J. Phys. Chem. A* **2001**, *105*, 6750−6756.

(4) Foresman, J. B.; Frisch, A. *Exploring Chemistry with Electronic Structure Methods*, 2nd ed.; Gaussian, Inc.: Pittsburgh, PA, 1993.

(5) (a) Becke, A. D. *Phys. Rev. A* **1988**, *38*, 3098−100. (b) Becke, A. D. *J. Chem. Phys.* **1993**, *98*, 5648−52. (c) Stephens, P. J.; Devlin, F. J.; Chabalowski, C. F.; Frisch, M. J. *J. Phys. Chem. A* **1994**, *98*, 11623.

(6) (a) Ochterski, J. W.; Petersson, G. A.; Wiberg, K. B. *J. Am. Chem. Soc.* **1995**, *117*, 11299−11308 and references therein. (b) Ochterski, J. W.; Petersson, G. A.; Montgomery, J. A. *J. Chem. Phys.* **1996**, *104*, 2598. (c) Montgomery, J. A.; Frisch, M. J.; Ochterski, J. W.; Petersson, G. A. *J. Chem. Phys.* **1999**, *110*, 2822−2827. (d) Petersson, G. A.; Ablaham, M. A. *J. Chem. Phys.* **1991**, *94*, 6081. (e) Petersson, G. A.; Tenseld, T. G.; Montgomery, J. A., Jr. *J. Chem. Phys.* **1991**, *94*, 6091. (f) Montgomery, J. A., Jr.; Ochterski, J. W.; Petersson, G. A. *J. Chem. Phys.* **1994**, *105*, 5900.

(7) Martin, J. M. L.; Oliveira, G. *J. Chem. Phys.* **1999**, *111*, 1843−1856.

(8) Houk, K. N.; Li, Y.; Evanseck, J. D. *Angew. Chem., Int. Ed. Engl.* **1992**, *31*, 682−708.

(9) For electrocyclic reactions of cyclobutene, see: (a) Rondan, N. G.; Houk, K. N. *J. Am. Chem. Soc.* **1985**, *107*, 2099−11. (b) Spellmeyer, D. C.; Houk, K. N. *J. Am. Chem. Soc.* **1988**, *110*, 3412−3416. (c) Spellmeyer, D. C.; Houk, K. N.; Rondan, N. G.; Miller, R. D.; Franz, L.; Fickes, G. N. *J. Am. Chem. Soc.* **1989**, *111*, 5356−5357. (d) Kallel, E. A.; Wang, Y.; Spellmeyer, D. C.; Houk, K. N. *J. Am. Chem. Soc.* **1990**, 6759−6763. For electrocyclic reactions of 1,3,5-hexatriene, see: (e) Evanseck, J. D.; Thomas, B. E., IV; Spellmeyer, D. C.; Houk, K. N. *J. Org. Chem.* **1995**, *60*, 7134−7141. For electrocyclic reactions of *o*-xylylenes, see: (f) Jefford, C. W.; Bernardinelli, G.; Wang, Y.; Spellmeyer, D. C.; Buda, A.; Houk, K. N. *J. Am. Chem. Soc.* **1992**, *114*, 1157−1165. For [1,5]-sigmatropic hydrogen shifts in 1,3-pentadiene and cyclopentadiene, see: (g) Rondan, H. G.; Houk, K. N. *Tetrahedron Lett.* **1984**, *24*, 2519−2522. (h) Jensen, F.; Houk, K. N. *J. Am. Chem. Soc.* **1987**, *109*, 3139−3140. For Cope rearrangement of 1,5-hexadiene, see: (i) Hrovat, D. A.; Borden, W. T. *J. Am. Chem. Soc.* **1990**, *112*, 2018−2019. (j) Houk, K. N.; Gustafson, S. M.; Black, K. A. *J. Am. Chem. Soc.* **1992**, *114*, 8565−8572. (k) Wiest, O.; Black, K. A.; Houk, K. N. *J. Am. Chem. Soc.* **1994**, *116*, 10336−10337. (l) Black, K. A.; Wilsey, S.; Houk, K. N. *J. Am. Chem. Soc.* **1998**, *120*, 5622−5627. (m) Hrovat, D. A.; Beno, B. R.; Lange, H.; Yoo, H. Y.; Houk, K. N.; Borden, W. T. *J. Am. Chem. Soc.* **1999**, *121*, 10529−10537. For Diels−Alder reactions of 1,3-butadiene and ethylene, see: (n) Caramella, P.; Domelsmith, L. N.; Houk, K. N. *J. Am. Chem. Soc.* **1977**, *99*, 4511−14. (o) Brown, F. K.; Houk, K. N. *Tetrahedron Lett.* **1984**, *25*, 4609−12. (p) Houk, K. N.; Lin, Y. T.; Brown, F. K. *J. Am. Chem. Soc.* **1986**, *108*, 554−556. (q) Li, Y.; Houk, K. N. *J. Am. Chem. Soc.* **1993**, *115*, 7478−7485. (r) Houk, K. N.; Yi, L.; Storer, J.; Raimondi, L.; Beno, B. *J. Chem. Soc., Faraday Trans.* **1994**, *90*, 1599−1604. (s) Storer, J. W.; Raimondi, L.; Houk, K. N. *J. Am. Chem. Soc.* **1994**, *116*, 9675−9683. (t) Goldstein, E.; Beno, B.; Houk, K. N. *J. Am. Chem. Soc.* **1996**, *118*, 6036−6043. (u) Beno, B. R.; Houk, K. N.; Singleton, D. A. *J. Am. Chem. Soc.* **1996**, *118*, 9984−9985. For Diels−Alder reactions of 1,3-cyclopentadiene and ethylene, see: (v) Houk, K.

N.; Loncharich, R. J.; Blake, J. F.; Jorgensen, W. L. *J. Am. Chem. Soc.* **1989**, *111*, 9172−9176. (x) Storer, J. W.; Raimondi, L.; Houk, K. N. *J. Am. Chem. Soc.* **1994**, *116*, 9675−9683. (y) Houk, K. N.; Wilsey, S. L.; Beno, B. R.; Kless, A.; Nendel, M.; Tian, J. *Pure Appl. Chem.* **1998**, *70*, 1947−1952. (z) Beno, B. R.; Wilsey, S.; Houk, K. N. *J. Am. Chem. Soc.* **1999**, *121*, 4816−4826. For [2 + 2 + 2] cycloreversion reactions of *cis*-triscyclopropacyclohexane and *cis*-triscyclobutacyclohexane, see: (a′) Sawicka, D.; Li, Y.; Houk, K. N. *J. Chem. Soc., Perkin Trans. 2* **1999**, 2349−2355. (b′) Sawicka, D.; Wilsey, S.; Houk, K. N. *J. Am. Chem. Soc.* **1999**, *121*, 864−865; also see reviews. (c′) Borden, W. T.; Loncharich, R. J.; Houk, K. N. *Annu. Rev. Phys. Chem.* **1988**, *39*, 213−236. (d′) Wiest, O.; Houk, K. N.; Black, K. A.; Thomas, B., IV *J. Am. Chem. Soc.* **1995**, *117*, 8594−8599. (e′) Wiest, O.; Houk, K. N. *Top. Curr. Chem.* **1996**, *183*, 1−24. (f′) Houk, K. N.; Beno, B. R.; Nendel, M.; Black, K.; Yoo, H. Y.; Wilsey, S.; Lee, J. K. *J. Mol. Struct.* **1997**, *398−99*, 169−179. (g′) Wiest, O.; Montiel, D. C.; Houk, K. N. *J. Phys. Chem. A* **1997**, *101*, 8378−8388. (h′) Wilsey, S.; Houk, K. N.; Zewail, A. H. *J. Am. Chem. Soc.* **1999**, *121*, 5772−5786.

(10) Roos, B. O.; Fulscher, M.; Malmquist, P. A.; Merchan, M.; Serrano-Andres, L. In *Quantum Mechanical Electronic Structure Calculations with Chemical Accuracy*; Langhoff, S. R., Ed.; Kluwer: Dordecht, 1995; p 357.

(11) KIEs studies: (a) Singleton, D. A.; Merrigan, S. R.; Liu, J.; Houk, K. N. *J. Am. Chem. Soc.* **1997**, *119*, 3385−3386. (b) Delmonte, A. J.; Haller, J.; Houk, K. N.; Sharpless, K. B.; Singleton, D. A.; Hang, C.; Strassner, T.; Thomas, A. A.; Leung, S. W.; Merrigan, S. R. *Tetrahedron* **2001**, *57*, 5149−5160.

(12) Lynch, B. J.; Fast, P. L.; Harris, M.; Truhlar, D. G. *J. Phys. Chem. A* **2000**, *104*, 4811−4815.

(13) Lynch, B. J.; Truhlar, D. G. *J. Phys. Chem. A* **2001**, *105*, 2936−41.

(14) Lynch, B. J.; Truhlar, D. G. *J. Phys. Chem. A* **2002**, *106*, 842−846.

(15) Lynch, B. J.; Truhlar, D. G. *J. Phys. Chem. A* **2003**, *107*, 3898−3906.

(16) Kang, J. K.; Musgrave, C. B. *J. Chem. Phys.* **2001**, *115*, 11040−11051.

(17) Senosiain, J. P.; Han, J. H.; Musgrave, C. B.; Golden, D. M. *Faraday Discuss.* **2001**, *119*, 173−189.

(18) Parthiban, S.; Oliveira, G.; Martin, J. M. L. *J. Phys. Chem. A* **2001**, *105*, 895−904.

(19) (a) Restrepo-Cossio, A. A.; Gonzalez, C. A.; Mari, F. *J. Phys. Chem. A* **1998**, *102*, 6993−7000. (b) Pai, S. V.; Chabalowski, C. F.; Rice, B. M. *J. Phys. Chem.* **1996**, *100*, 15379−15382. (c) Baker, J.; Andzelm, J.; Muir, M.; Taylor, P. R. *Chem. Phys. Lett.* **1995**, *237*, 53−60. (d) Durant, J. *Chem. Phys. Lett.* **1996**, *256*, 595−602.

(20) (a) Dinadayalane, T. C.; Vijaya, R.; Smitha, A.; Sastry, N. G. *J. Phys. Chem.* **2002**, *106*, 1627−1633. (b) Vijaya, R.; Dinayalane, T. C.; Sastry, G. N. *J. Mol. Struct.* **2002**, *589−590*, 291−299.

(21) Handy, N. C.; Cohen, A. *J. Mol. Phys.* **2001**, *99*, 403.

(22) Hoe, W.-M.; Cohen, A. J.; Handy, N. C. *Chem. Phys. Lett.* **2001**, *341*, 319.

(23) Baker, J.; Pulay, P. *J. Chem. Phys.* **2002**, *117*, 1441−1449.

(24) Cooper, W.; Walters, W. D. *J. Am. Chem. Soc.* **1958**, *80*, 4220−4224.

(25) Carr, R. W.; Walters, W. D. *J. Phys. Chem.* **1965**, *69*, 1073−1075.

(26) Hauser, W. P.; Walters, W. D. *J. Phys. Chem.* **1968**, *67*, 1328−1333.

(27) Estimated using heat of formations of cyclobutene ($H_f = 37.5 \pm 0.4$ kcal/mol) and 1,3-butadiene ($H_f = 26.00 \pm 0.19$ kcal/mol and $26.75 \pm 0.23$ kcal/mol). Data from NIST Standard Reference Database. http://webbook.nist.gov/chemistry.

(28) Benson, S. W.; O'Neal, H. E. *Natl. Stand. Ref. Data Ser., Natl. Bur. Stand.* **1970**, No 21.

(29) (a) Danti, A. *J. Chem. Phys.* **1957**, *27*, 1227. (b) Aston, J. G.; Szazs, G.; Wooley, H. W.; Brickwedde, F. G. *J. Chem. Phys.* **1946**, *14*, 67−79.

(30) Lewis, K. E.; Steiner, H. *J. Chem. Soc.* **1964**, 3080.

(31) Estimated using heat of formations of cyclohexene ($H_f = 25.019$ kcal/mol) and 1,3,5-hexatriene ($H_f = 41.15$ kcal/mol). Data from NIST Standard Reference Database. http://webbook.nist.gov/chemistry.

(32) Roth, W. R.; Biermann, M.; Dekker, H.; Jochems, R.; Mosselman, C.; Herman, H. *Chem. Ber.* **1978**, *111*, 3892−3903.

(33) Roth, W. R. *Chimia* **1966**, *229*, 20.

(34) Roth, W. R.; Konig, J. *Ann. Chem.* **1966**, *699*, 24.

(35) Roth, W. R. *Tetrahedron Lett.* **1964**, 1009−1013.

(36) Doering, W. E.; Toscano, V. G.; Beasley, G. H. *Tetrahedron* **1971**, *27*, 5299−5306.

(37) Rowley, D.; Steiner, H. *Discuss. Faraday Soc.* **1951**, *27*, 5299−5306.

(38) Uchiama, M.; Tamioka, T.; Amano, A. *J. Phys. Chem.* **1964**, *68*, 1878−1881.

(39) Kraus, M.; Vavruska, M.; Bazant, V. *Collect. Czech. Chem. Commun.* **1957**, *22*, 484.

(40) Smith, S. R.; Gordon, A. S. *J. Phys. Chem.* **1961**, *65*, 1124.

(41) Estimated using heat of formations of 1,3-butadiene ($H_f$ = 26.00 ± 0.19 kcal/mol and 26.75 ± 0.23 kcal/mol), ethylene ($H_f$ = 12.54 kcal/mol), and cyclohexene ($H_f$ = −1.03 ± 0.23 kcal/mol). Data from NIST Standard Reference Database. http://webbook.nist.gov/chemistry.

(42) Walls, R.; Wells, J. M. *J. Chem. Soc., Perkin Trans. 2* **1976**, 52−55.

(43) Herndon, W. C.; Cooper, W. B.; Chambers, M. J. *J. Phys. Chem.* **1964**, *79*, 2016−2018.

(44) Roquitte, B. C. *J. Phys. Chem.* **1965**, *69*, 1351−1354.

(45) Kiefer, J. H.; Kumaran, S. S.; Sundaram, S. *J. Chem. Phys.* **1993**, *99*, 3531−3541.

(46) Balcioglu, N.; Guner, V. *Instrum. Sci. Technol.* **2001**, *29*, 193−200.

(47) Walsh, R.; Wells, J. M. *J. Chem. Thermodyn.* **1976**, *8*, 55−60.

(48) Harkness, J. B.; Kistiakowsky, G. B.; Mears, W. H. *J. Chem. Phys.* **1937**, *5*, 792.

(49) Benford, G. A.; Wassermann, A. *J. Chem. Soc.* **1939**, 362, 367, 371.

(50) (a) Estimated using heat of formations of cyclopentadiene ($H_f$ = 25.04 ± 0.3 kcal/mol for liquid phase, 31.82 ± 0.3 kcal/mol for gas phase) and dicyclopentadiene ($H_f$ = 31.6 ± 0.5 kcal/mol for liquid phase, 42.2 ± 0.6 kcal/mol for gas phase). (b) Turnbull, A. G.; Hull, H. S. *Aust. J. Chem.* **1968**, *21*, 1789−97. (c) Herndon, W. C.; Grayson, C. R.; Manion, J. M. *J. Org. Chem.* **1967**, *32*, 526−529.

(51) Schultze, G. R. *Oel, Kohle, Erdoel, Teer* **1938**, *14*, 113.

(52) Benford, G. A.; Kaufmann, H.; Khambata, B. S.; Wassermann, A. *J. Chem. Soc.* **1939**, 38.

(53) Flammersheim, H. J.; Opfermann, J. *Thermochim. Acta* **1997**, *337*, 149−153.

(54) Kistiakowsky, G. B.; Mears, W. H. *J. Am. Chem. Soc.* **1936**, *58*, 1060.

(55) Herndon, W. C.; Grayson, C. R.; Manion, J. M. *J. Org. Chem.* **1967**, *32*, 526−529.

(56) Spielman, W.; Fick, H. H.; Meyer, L. U.; de Meijere, A. *Tetrahedron Lett.* **1976**, *45*, 4057.

(57) (a) Maas, M.; Lutterbeck, M.; Hunkler, D.; Prinzbach, H. *Tetrahedron Lett.* **1983**, *24*, 2143−2149. (b) Mohler, D. L.; Vollhardt, R. P. C.; Wolf, S. *Angew. Chem., Int. Ed. Engl.* **1990**, *29*, 1151−1154.

(58) Liu, Y. P.; Lynch, G. C.; Truong, T. N.; Lu, D. H.; Truhlar, D. G.; Garrett, B. C. *J. Am. Chem. Soc.* **1993**, *115*, 2408−2415.

(59) Frisch, M. J.; Trucks, G. W.; Schlegel, H. B.; Scuseria, G. E.; Robb, M. A.; Cheeseman, J. R.; Zakrzewski, V. G.; Montgomery, J. A., Jr.; Stratmann, R. E.; Burant, J. C.; Dapprich, S.; Millam, J. M.; Daniels, A. D.; Kudin, K. N.; Strain, M. C.; Farkas, O.; Tomasi, J.; Barone, V.; Cossi, M.; Cammi, R.; Mennucci, B.; Pomelli, C.; Adamo, C.; Clifford, S.; Ochterski, J.; Petersson, G. A.; Ayala, P. Y.; Cui, Q.; Morokuma, K.; Malick, D. K.; Rabuck, A. D.; Raghavachari, K.; Foresman, J. B.; Cioslowski, J.; Ortiz, J. V.; Stefanov, B. B.; Liu, G.; Liashenko, A.; Piskorz, P.; Komaromi, I.; Gomperts, R.; Martin, R. L.; Fox, D. J.; Keith, T.; Al-Laham, M. A.; Peng, C. Y.; Nanayakkara, A.; Gonzalez, C.; Challacombe, M.; Gill, P. M. W.; Johnson, B. G.; Chen, W.; Wong, M. W.; Andres, J. L.; Head-Gordon, M.; Replogle, E. S.; Pople, J. A. *Gaussian 98*, revision A.9; Gaussian, Inc.: Pittsburgh, PA, 1998.

(60) Hehre, W. J.; Radom, L.; Schleyer, P. v.; Pople, J. A. *Ab initio Molecular Orbital Theory*; John Wiley & Sons: New York, 1986.

(61) Szabo, A.; Ostlund, N. S. *Modern Quantum Chemistry*; McGraw-Hill: New York, 1989. Also see references therein.

(62) (a) Moller, C.; Plesset, M. S. *Phys. Rev.* **1934**, *46*, 618. (b) Rachavachari, K.; Anderson, J. B. *J. Phys. Chem.* **1996**, *100*, 12960.

(63) Ross, B. O. In *Ab initio Methods in Quantum Chemistry*; Lawley, K. P., Ed.; Wiley: New York, 1987; Vol. 2, p 399.

(64) (a) Shepard, R. In *Ab initio Methods in Quantum Chemistry*; Lawley, K. P., Ed.; Wiley: New York, 1987; Vol 1. (b) Bernardi, F.; Olivucci, M.; McDouall, J. J.; Robb, M. A. *J. Chem. Phys.* **1988**, *89*, 6365.

(65) (a) Wolinski, K.; Pulay, P. J. *J. Chem. Phys.* **1989**, *90*, 3647. (b) Murphy, R. B.; Messmer, R. P. *Chem. Phys. Lett.* **1991**, *183*, 443. (c) Andersson, K.; Malmquist, P. A.; Roos, B. O. *J. Chem. Phys.* **1992**, *96*, 1218.

(66) Andersson, K.; Roos, B. O. In *Modern Electronic Structure Theory*; Yarkany, D. R., Ed.; World Scientific: Singapore, 1995; p 55.

(67) (a) Kohn, W.; Sham, L. J. *Phys. Rev. A* **1965**, *140*, 133. (b) Becke, A. D. *Phys. Rev. A* **1998**, *38*, 3098. (c) Becke, A. D. *J. Chem. Phys.* **1993**, *98*, 5648.

(68) (a) Vosko, S. H.; Wilk, L.; Nusair, M. *Can. J. Phys.* **1980**, *58*, 1200. (b) Lee, C.; Yang, W.; Pair, R. G. *Phys. Rev. B* **1988**, *37*, 785. (c)

Perdew, J. P.; Zunger, A. *Phys. Rev. B* **1981**, *23*, 5048. (d) Perdew, J. P. *Phys. Rev. B* **1986**, *33*, 8822. (e) Perdew, J. P; Wang, Y. *Phys. Rev. B* **1992**, *45*, 13244.

(69) (a) Parr, R. G.; Yang, W. *Density-Functional Theory of Atoms and Molecules*; Oxford University Press: New York, 1989. (b) Koch, W.; Halthausen, M. C. *A Chemist's Guide to Density Functional Theory*; Wiley-VCH: New York, 1999. (c) Labanowski, J. W.; Andzelm, J. *Density Functional Methods in Chemistry*; Springer: New York, 1991. (d) *Modern Density Functional Theory*; Seminario, J. M., Politzer, P., Eds.; Elsevier: Amsterdam, 1995.

(70) (a) Becke, A. D. *J. Chem. Phys.* **1992**, *96*, 2155−2160. (b) Becke, A. D. *J. Chem. Phys.* **1992**, *97*, 9173−9177. (c) Becke, A. D. *J. Chem. Phys.* **1993**, *98*, 5648−5652.

(71) (a) Stephens, P. J.; Devlin, F. J.; Chabalowski, C. F.; Frisch, M. J. *J. Phys. Chem.* **1994**, *98*, 11623. (b) Stephens, P. J.; Devlin, F. J.; Ashvar, C. S.; Bak, K. L.; Taylor, P. R.; Frisch, M. J. *ACS Symp. Ser.* **1996**, *629*, 105.

(72) Burke, K.; Perdew, J. P.; Wang, V. In *Electronic Density Functional Theory: Recent Progress and New Directions*; Dobsin, J. F., Vignale, G., Das, M. P., Eds.; Plenum: New York, 1998.

(73) Lynch, B. J.; Fast, P. L.; Patton, L. F.; Harris, M.; Truhlar, D. G. *J. Phys. Chem. A* **2001**, *104*, 21.

(74) Andersson, K.; Malmqvist, P.-A.; Roos, B. O. *J. Chem. Phys.* **1992**, *96*, 1218.

(75) Andersson, K.; Barysz, M.; Bernhardsson, A.; Blomberg, M. R. A.; Cooper, D. L.; Fleig, T.; Fülscher, M. P.; de Graaf, C.; Hess, B. A.; Karlström, G.; Lindh, R.; Malmqvist, P.-Å.; Neogrády, P.; Olsen, J.; Roos, B. O.; Sadlej, A. J.; Schimmelpfennig, B.; Schütz, M.; Seijo, L.; Serrano-Andrés, L.; Siegbahn, P. E. M.; Stålring, J.; Thorsteinsson, T.; Veryazov, V.; Widmark, P.-O. *MOLCAS* Version 5.0; Lund University: Sweden, 2001.

(76) (a) Gordon, M. S. *Chem. Phys. Lett.* **1980**, *76*, 163. (b) Krishnan, R.; Binkley, J. S.; Seeger, R.; Pople, J. A. *J. Chem. Phys.* **1980**, *72*, 690.

(77) Hess, B. A.; Schaad, L. J. *J. Am. Chem. Soc.* **1983**, *105*, 7185−7186.

(78) Hess, B. A., Jr.; Schaad, L. J.; Pancir, J. *J. Am. Chem. Soc.* **1985**, *107*, 149−154.

(79) Bachrach, S. M. *J. Org. Chem.* **1993**, *58*, 5414−5421.

(80) Staroverov, V. N.; Davidson, E. R. *J. Mol. Struct.* **2001**, *573*, 81−89.

(81) Barone, V.; Arnaud, R. *Chem. Phys. Lett.* **1996**, *251*, 393−99.

(82) Barone, V.; Arnaud, R. *J. Chem. Phys.* **1997**, *106*, 8727−8732.

(83) Huei, C.; Tsai, L. C.; Hu, W. P. *J. Phys. Chem. A* **2001**, *105*, 9945−53.

(84) Branchadell, V. *Int. Quantum Chem.* **1997**, 381−388.

(85) Saettal, N. J.; Wiest, O. *J. Org. Chem.* **2000**, *65*, 2331−2336.

(86) Jia, H.; Schleyer, P. R. *J. Chem. Soc., Faraday Trans.* **1994**, *90*, 1559−1567.

(87) Alkorta, I.; Elguero, J. *J. Chem. Soc., Perkin Trans. 2* **1998**, 2497−2503.

(88) Jiao, H.; Schleyer, R. *Angew. Chem., Int. Ed. Engl.* **1995**, *34*, 334−337.

(89) Froese, R. D.; Coxon, J. M.; West, C. S.; Morokuma, K. *J. Org. Chem.* **1997**, *62*, 6991−6996.

(90) Froese, R. D.; Humber, S.; Svenson, M.; Morokuma, K. J. *J. Phys. Chem. A* **1997**, *101*, 227.

(91) Park, Y. S.; Lee, B. S.; Lee, I. *New J. Chem.* **1999**, *23*, 707−715.

(92) Sakai, S. *THEOCHEM* **1999**, *283*, 461−462.

(93) Sakai, S. H.; Takane, S. *J. Phys. Chem. A* **1999**, *103*, 2878−2882.

(94) Sakai, S. *J. Phys. Chem.* **2000**, *104*, 11615.

(95) Sakai, S. *J. Phys. Chem. A* **2000**, *104*, 922−927.

(96) Jursic, B. S. *J. Mol. Struct.* **1998**, *423*, 189−194.

(97) Jursic, B.; Zadrovski, Z. *J. Chem. Soc., Perkin Trans 2* **1995**, 1223.

(98) Bradley, A. Z.; Kociolek, M. G.; Johnson, R. P. *J. Org. Chem.* **2000**, *65*, 7134−7138.

(99) Caramella, P.; Quadrelli, P.; Toma, L. *J. Am. Chem. Soc.* **2002**, *124*, 1130−1131.

(100) Sawicka, D.; Li, Y.; Houk, K. N. *J. Chem. Soc., Perkin Trans. 2* **1999**, 2349−2355.

(101) Sawicka, D.; Wilsey, S.; Houk, K. N. *J. Am. Chem. Soc.* **1999**, *121*, 864−865.

(102) Guner, V.; Houk, K. N.; unpublished results.

(103) Musgrave, C.; private communication. C. S. Warner and P. v. R. Schleyer have informed us of similar improvements in KMLYP results with larger basis sets.